File

SSC-168

Rolling History in Relation to The Toughness of Ship Plate

by

B. M. KAPADIA AND W. A. BACKOFEN

SHIP STRUCTURE COMMITTEE

Copies available from Secretary, Ship Structure Committee,
U. S. Coast Guard Headquarters, Washington, D. C. 20226

SHIP STRUCTURE COMMITTEE

MEMBER AGENCIES:

BUREAU OF SHIPS, DEPT. OF NAVY
MILITARY SEA TRANSPORTATION SERVICE, DEPT. OF NAVY
UNITED STATES COAST GUARD, TREASURY DEPT.
MARITIME ADMINISTRATION, DEPT. OF COMMERCE
AMERICAN BUREAU OF SHIPPING

ADDRESS CORRESPONDENCE TO:

SECRETARY
SHIP STRUCTURE COMMITTEE
U. S. COAST GUARD HEADQUARTERS
WASHINGTON 25, D. C.

May 1965

Dear Sir:

Herewith is a copy of SSC-168 entitled Rolling History in Relation to the Toughness of Ship Plate by B. M. Kapadia and W. A. Backofen. This is the final report on a project sponsored by the Ship Structure Committee at the Massachusetts Institute of Technology to determine the relationship of mill-rolling practice to metallurgical structure and properties of ship plate.

In sponsoring this research project, the Ship Structure Committee, received guidance and review from the National Academy of Sciences through its Ship Hull Research Committee, and a Project Advisory Committee SR-147, "Mill-Rolling Practice," established specifically for liaison with the principal investigator. The Academy undertakes this research advisory service to the Ship Structure Committee through a contract arrangement.

Comments on this report would be welcomed and should be addressed to the Secretary, Ship Structure Committee.

Sincerely yours,

JOHN B. OREN
Rear Admiral, U. S. Coast Guard
Chairman, Ship Structure
Committee

SSC-168

ROLLING HISTORY IN RELATION TO THE TOUGHNESS OF SHIP PLATE

by

B. M. Kapadia and W. A. Backofen
Massachusetts Institute of Technology

Prepared for
THE SHIP STRUCTURE COMMITTEE
Project SR-147, "Mill Rolling Practice"

under

Department of the Navy
Bureau of Ships Contract NObs-88282

Washington, D. C.
National Academy of Sciences-National Research Council
May 1965

ABSTRACT

Plates of ABS Class-B and Class-C steel were rolled with different temperature-reduction schedules to observe effects of processing history on final structure and properties. Each class was finished at a constant thickness (1-1/2-inch for Class B; 1-1/4-inch for Class C) following both isothermal and non-isothermal schedules with reductions from 15 percent to 60 percent and temperatures in the range 1250°F (677°C) to 2000°F (1093°C). The principal measurements for toughness evaluation were the 15 foot-pound V-notch Charpy, the 50 percent-fibrous Charpy, and the tensile-ductility transition temperatures.

Effects were divided into two basic categories, one concerned entirely with ferrite grain size, the other with various extra-grain-size details of structure and composition. The most significant improvements in toughness were the result of ferrite grain-size refinement. The notch toughness of both steels was increased equally for this reason as rolling temperature was lowered to 1450°F (788°C).

The superior toughness of Class C at constant grain size was an example of an extra-grain-size effect of composition. Normalizing of Class B plates after rolling produced Widmanstätten structure and some embrittlement which was interpreted as an apparent extra-grain-size effect of this particular heat treatment. Mechanical fibering was studied with techniques that included electron microscopy, but the contribution of microfissuring effects to toughness was too subtle for observation. Embrittlement from residual cold work as a consequence of low-temperature finishing was also identified. Results of heat treatment after rolling were studied in detail; of special interest was a pronounced increase in transition temperature from sub-critical annealing, which has been related in some measure to carbide spheroidization.

Possibilities for further toughness improvement by control of rolling history have been discussed.

CONTENTS

INTRODUCTION

Some degree of controlled shape change is invariably a goal in processing. Associated with this, however, there is a capacity for control of properties which is not always realized. In deformation processing, the latter control must be based entirely on a regulation of structure in its various forms. More specifically, in the hot rolling of steel ship plate, there are several possibilities for altering structure so as to control, and even to improve, the notch toughness of the resulting product. Whether they ever find practical application will be determined largely by other, economic factors. In the U.S.A., the facilities for steel plate rolling are in most plants of a type that substantial improvements would be the prerequisite for any serious consideration of change in practice.

At least three such possibilities have been recognized, each relating to a different detail of material structure. One is based on ferrite grain size, which acts to depress transition temperature as it is made smaller.[1-6] The improvement varies with the type of test and the criterion for evaluating transition temperature,[7-9] but it has been found that the temperature defined by 15 foot-pound energy absorption in the Charpy V-notch impact test is lowered by an amount somewhere in the range 15-25°F (8-14°C) for each unit of increase on the ASTM grain-size scale.[4,6,9] No other variable has such a potent effect, so that reduction of ferrite grain size (or increase in grain-size number) is the most attractive, if not fully explored, method of microstructural toughening. Currently, the grain size in rolled plates is rarely finer than ASTM No. 8. Abroad, however, controlled-rolling processes have been devised in which temperature-reduction schedules are regulated so as to finish at lower-than-normal temperatures (near the upper-critical), with the result that grain size is smaller by about 1 ASTM unit and transition temperature is lowered accordingly.[10,11] A handicap in the eventual planning of even more sophisticated control lies in the limited understanding of kinetics and structural change in hot working.

With major importance attached to ferrite grain size, other possibilities for toughness regulation are conveniently labelled as "extra-grain-size" in origin. The second of the three, in this category, involves the mechanically aligned fiber-like structure of included particles, pores, and other weak interfaces inherent in wrought materials. Such a structure is basically responsible for an anisotropy in fracturing characteristics.[12-15] When a crack travels by cutting across the fiber, it has been shown that triaxiality in regions of stress concentration at crack tips may be relaxed by local (micro-scale) separations (or fissuring) between the less strongly cohering fiber elements.[6,8] In that way, more intense fibering or greater fracturing anisotropy may have a toughening influence. Lower finishing temperature has been found to favor the trend.[6,8] Again, the amount of toughening as measured by a drop in transition temperature is different, depending upon criterion applied.[8] However, it is clear that the effect is not nearly so marked as that of grain size. Quantitative estimates are difficult to find, but statistically derived formulas from van der Veen,[7] for calculation of transition temperature, contain terms suggesting that the fiber effect is roughly an order of magnitude less than that of grain size.

TABLE I. CHEMICAL COMPOSITION.

Component	Percent by Weight, in	
	ABS Class B Steel	ABS Class C Steel
C	0.20	0.23
Mn	0.93	0.66
P	0.012	0.014
S	0.031	0.03
Si	0.02	0.17
Cu	0.05	
Ni	0.06	
Cr	0.03	
Mo	0.04	
V	< 0.005	
Ti	< 0.005	
Al (Acid Sol.)	0.002	0.029
Al (Total)	0.006	0.033
N (Acid Sol.)	0.007	
N (Total)	0.008	0.004

Still a third possibility is associated with residual cold work that may be introduced in attempting to schedule low-temperature passes for grain-size refinement and fiber development. Its contribution ought to be strongly negative,[16,17] but control to avoid its presence should be important in producing optimum microstructure.

With such background, generally known but not yet fully detailed, plans were made to evaluate structure-property relationships in a number of systematically rolled plates of ship-hull steels. Schedules were arranged to cover a variety of temperature-reduction sequences, and in view of the recognized bearing of measurement criterion on toughness observed, both unnotched tension and Charpy impact tests were planned. The outcome of that work is related here.

MATERIALS AND EXPERIMENTAL PROCEDURES

Plates were rolled from steels of ABS Class B and Class C specifications.[18] Class B is a semi-killed steel, Class C a fine-grain killed steel. Chemical analyses are given in Table I.

TABLE II. PROCESSING HISTORIES.

Numbers within the table identify plates rolled according to the different schedules.

ABS Class B, 1-1/2-inch final thickness

Reduction, %	Isothermal reduction at (°F)				Non-isothermal reduction, finishing at (°F)		
	1250	1450	1650	1950	1250	1455	1595
15	25	10	19	2	--	--	--
30	9	13	16	8	1*	22*	12*
60	23	20	11	6	--	--	--

* Non-isothermal reduction schedules comprising six equal passes with the temperature dropping approximately 40°F per pass to the finishing level. The rolling schedule of plate 12 was nearly that of conventional industrial practice in the U.S.A., while the schedule of plate 22 represented approximately the controlled rolling practice of certain mills in Europe.[19]

ABS Class C, 1-1/4-inch final thickness

Reduction, %	Isothermal reduction at (°F)			Non-isothermal reduction, finishing at 1800°F
	1600	1800	2000	
20	9	8	7	----
50	4	3	2	12**

** Standard industrial practice with the last 50% reduction being made on a falling temperature scale, from 2090°F to 1800°F.

Rolling Histories: Class B plates were rolled according to 15 different schedules (Table II and IA*). Preliminary rolling of 6-inch-thick slabs was carried out above 2100°F to establish the proper initial thicknesses for developing the same final thickness of 1-1/2-inch. Following the slab-sizing reductions, plates were allowed to cool in air to selected lower temperatures before further rolling. Twelve of the final schedules were nominally isothermal, each involving 6 equal drafts for total reductions of 15, 30 and 60 percent at 1950°F (1066°C), 1650°F (899°C), 1450°F (788°C), and 1250°F (677°C). Each of the remaining three schedules accomplished total reductions of 30 percent, again in 6 equal passes, with the temperature dropping approximately 40°F per pass to the final values of 1595°F (868°C), 1455°F (790°C), and 1250°F (677°C). A schematic plot of the rolling temperature vs. cumulative percent reduction for all plates reduced 30 percent is given in Figure 1. The controlled-rolling practice of the Royal Netherlands Blast Furnaces and Steelworks[11-19] was the model for the non-isothermal schedules; a dashed line in Figure 1 is representative of such practice. The temperature-reduction trend in more conventional practice is also noted in Figure 1.

---

* The letter designation refers to a table or figure in the Appendix.

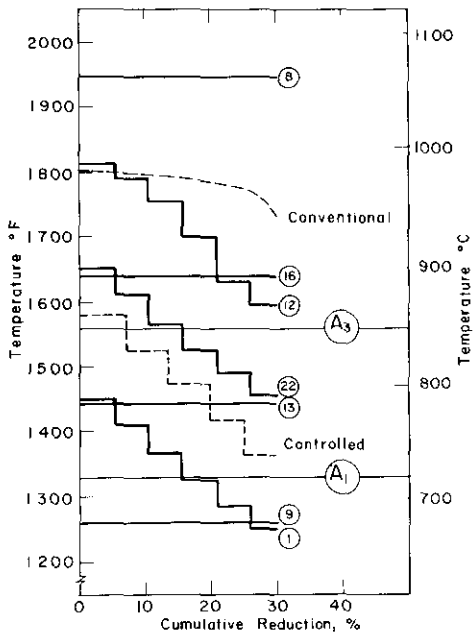

Fig. 1. Rolling Temperature vs. Cumulative Percent Reduction for ABS Class B Plates Rolled 30% with Isothermal and Non-isothermal Reductions. Numbers identify plates described in Table II. A_1 and A_3 are the lower and upper critical temperatures, respectively. Dashed lines represent a conventional reduction schedule and the controlled rolling practice of Royal Netherland Blast Furnaces and Steelworks, Holland. (19)

Seven different rolling schedules were selected for the Class C plates (Table II and IA). Six were nominally isothermal as before, with total reductions of 20 and 50 percent at 2000°F (1093°C), 1800°F (982°C), and 1600°F (871°C). The remaining plate was rolled according to a conventional industrial practice. All plates were finished at a thickness of 1-1/4-inch. In this case, however, the slabs were cooled to room temperature after preliminary sizing, reheated to 2050°F, and then air-cooled to the different final-rolling temperatures.

Various heat treatments involving normalizing, annealing, and homogenizing were performed on selected plates after rolling and prior to mechanical testing. Details of the treatments and designations of the heat-treated plates are given in Table III.

Ferrite Grain Size: With the method of lineal analysis, a determination was made in each plate of the average linear intercept between ferrite-ferrite or ferrite-pearlite boundaries along the three reference directions: rolling (R), transverse (T), and thickness (Z).

In one approach to establishing grain size, the over-all mean, $\bar{\alpha}$, was obtained as the cube root of the product of the three intercepts. Assuming the ferrite grains to be Kelvin equi-edged tetrakaidekahedrons which completely fill space, the number of ferrite grains per unit volume of ferrite is calculable from:[20,21]

$$N_V = \frac{0.4263}{\bar{\alpha}^3}$$

The ASTM grain-size numbers could then be derived from $\log_{10} N_V$ using a tabulation by Rutherford et al.[21]

TABLE III. DETAILS OF HEAT TREATMENT.

ABS CLASS B

Plate Identification Number	Treatment	Designation
2, 9, 10 16, 20, 25	1650°F (899°C), 1-1/2 hr., air-cooled ... (Normalize)	2a,9a,10a* 16a,20a,25a
10 20	1725°F (940°C), 2-1/2 hr., furnace-cooled ... (Full Anneal) 1725°F (940°C), 5 hr., furnace-cooled ... (Full Anneal)	10B* 20C
8 9 9, 16 8 8	1250°F (677°C), 1 hr., air-cooled ... (Subcritical Anneal) 1250°F (677°C), 2 hr., air-cooled ... (Subcritical Anneal) 1250°F (677°C), 2 hr., furnace-cooled ... (Subcritical Anneal) 1250°F (677°C), 10 hr., air-cooled ... (Subcritical Anneal) 1250°F (677°C), 10 hr., furnace-cooled ... (Subcritical Anneal)	8e 9f 9F,16F 8g 8G
8 8H 8H	2200°F (1200°C), 20 hr., slowly cooled** ... (Homogenize) 1650°F (899°C), 1-1/2 hr., air-cooled; repeated ... (Double Normalize) 1650°F (899°C), 1-1/2 hr., air-cooled (Normalize); followed by 1650°F (899°C), 1-1/2 hr., furnace-cooled (Full Anneal)	8H 8Haa 8HaA

ABS CLASS C

Plate Identification Number	Treatment	Designation
4, 7	1650°F (899°C), 1-1/2 hr., air-cooled ... (Normalize)	4a, 7a
4, 7	1250°F (677°C), 2 hr., air-cooled ... (Subcritical Anneal)	4f, 7f

* Small letters represent air-cooling and capital letters furnace-cooling. The average rates of air- and furnace-cooling through the transformation range were approximately 60°F (33°C) per minute and 4.5°F (2.5°C) per minute, respectively.

** Furnace-cooled at a rate of approximately 1.8°F (1.0°C) per minute down to about 1200°F (649°C), and then air-cooled to room temperature.

An alternative grain-size evaluation was based only upon average intercepts in the T and Z directions, the reason being that fracture in conventionally oriented Charpy specimens propagates mainly in the T-Z plane. However, the difference between T-Z and R-T-Z values was never more than 0.25 ASTM units (R-T-Z giving the smaller ASTM number) except in plate B-23 where the R-T-Z value was smaller by about 0.85 units. Charpy test results have been related in what follows to the T-Z or "fracture-plane" grain size.

Pearlite-patch Size: Lineal analysis along the three reference directions was similarly made to define the pearlite-patch size. The pearlite regions assumed various irregular shapes, and hence the mean pearlite lineal intercept (based on the three unidirectional averages) was taken as the most appropriate parameter for patch size. The volume fraction was given directly by the ratio of total pearlite intercept to the total traverse in ferrite and pearlite.

Inclusion Fibering: To provide at least a relative indication of the intensity of inclusion fibering, all inclusions above a certain size were counted on polished and unetched surfaces using a micrometer microscope with travelling stage. The lower size limit was set at 0.02 millimeter, and the total count, q, included those intersected by an imaginary 100 millimeter line in the R-Z plane along the Z direction; the method originates with van der Veen.[7] The quantity, q, is thus determined by the size and shape of individual inclusions, as well as by the amount of included material. For given inclusion content, a greater degree of inclusion elongation (or fibering) is reflected in a higher q value.

Tensile Testing: Tensile tests were made in rolling (R) and thickness (Z) directions on all as-rolled Class B plates from room temperature down to -405°F (-243°C), using 20 or more specimens per plate and test direction. Room-temperature tests were also made on all as-rolled Class C, and some of the heat-treated plates. Plain cylindrical specimens with shoulders for gripping were machined to a gage diameter of 0.25 inch and length about 0.875 inch, with total specimen length of 1-1/2-inch (Class B) or 1-1/4-inch (Class C). Apparatus and test procedure have been described elsewhere.[6] Lower-yield stress, ultimate tensile strength, and the true stress at fracture were computed from autographic load vs. elongation records, the pulling speed being about 0.05 inch/minute. The fracture-stress calculation, and that for true fracture-strain as well, required the cross-sectional area at fracture;* this was obtained by rejoining the halves of a broken specimen and measuring the minimum diameter on an optical comparator. A mean diameter was used if specimens became elliptical during extension. For all as-rolled Class B plates, the lower yield stress σ_y, true fracture stresses σ_R and σ_Z, and true fracture strains, ϵ_R and ϵ_Z, (R and Z identifying directions of measurement) were plotted against test temperature in obtaining data presented below.

Charpy Impact Testing: V-notch Charpy tests were made on all as-rolled and heat-treated plates. The 15 foot-pound (T_{V-15}) and 50 percent fibrous ($T_{V-50\%}$) transition temperatures were determined by testing about 25-30 specimens per plate, with specimen length along the rolling direction and notch in the thickness direction. Precision was estimated to be $\pm$ 10.5°F (6°C) and $\pm$ 18°F (10°C) for T_{V-15} and $T_{V-50\%}$, respectively, with a confidence of 95 percent. Tests were also made on some plates with specimen length along the transverse direction. Complete experimental details and stastical analysis of the results are given in the Appendix.

Microstructural Examination: Metallographically polished and etched surfaces were examined for microstructural details. Comparisons were made of interlamellar spacings of the pearlite in all Class B plates. The amount of spheroidization during subcritical annealing was estimated visually and noted as a fraction of the total cementite content. Fracture surfaces and microcracks were also studied on sectioned tensile and Charpy bars tested near the transition temperatures.

---

* Formulas are: σ (true fracture stress) = P_f/A_f and ϵ (true fracture strain) = ln (A_o/A_f) where P_f and A_f are load and cross-sectional area at fracture, respectively, and A_o is the original area of cross section.

Observations on inclusions with light microscopy were limited to a diameter of about 1 μ. Below this limit, to about 0.05 μ, electron microscopy was used to examine inclusion structure and other details of fracture on selected surfaces treated with a two-stage technique for producing chromium-shadowed, negative carbon replicas. Details are found in the Appendix.

RESULTS

Rolling schedules were selected with the intention of developing a wide range of structure, especially of ferrite grain size and of the mechanical fibering responsible for fracturing anisotropy. The limited success in these efforts to manipulate structure is evident from Figures 2 and 3. The ferrite grain-size variation was only 2 ASTM units, from about 6.4 to 8.65, and q was changed relatively little, except by the heaviest reductions. Further details are given in the Appendix.

A. Structure

Ferrite Grain Size: It is clear from recent studies that grain size after recrystallization during hot working is determined in large measure by the size of the deformed parent grains.[22,23] The reason is that new grains tend to be nucleated along the boundaries of the old. Since all plates (of each class) were at the same austenitizing temperature before rolling, all ought to have had about the same initial austenite grain size. Therefore, the final austenite grain size of plates rolled above the critical range could have been more nearly alike than might be expected in view of the wide variations in rolling history. This would have led, in turn, to only modest differences in the ultimate ferrite grain size.

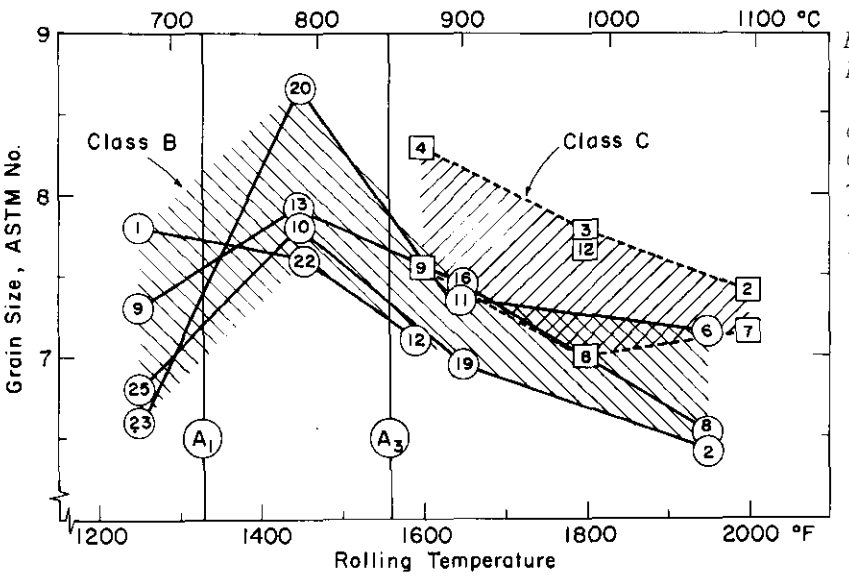

Fig. 2. Dependence of Ferrite Grain Size (R-T-Z) on Rolling History of Class B (O) and Class C (□) Plates. Numbers identify plates described in Table II. Points representing the same percent reduction are interconnected. Plates rolled according to non-isothermal practice (B-12, -22, -1; C-12) are represented by the temperature of the finishing pass. A_1 and A_3 are the lower and upper critical temperatures, respectively.

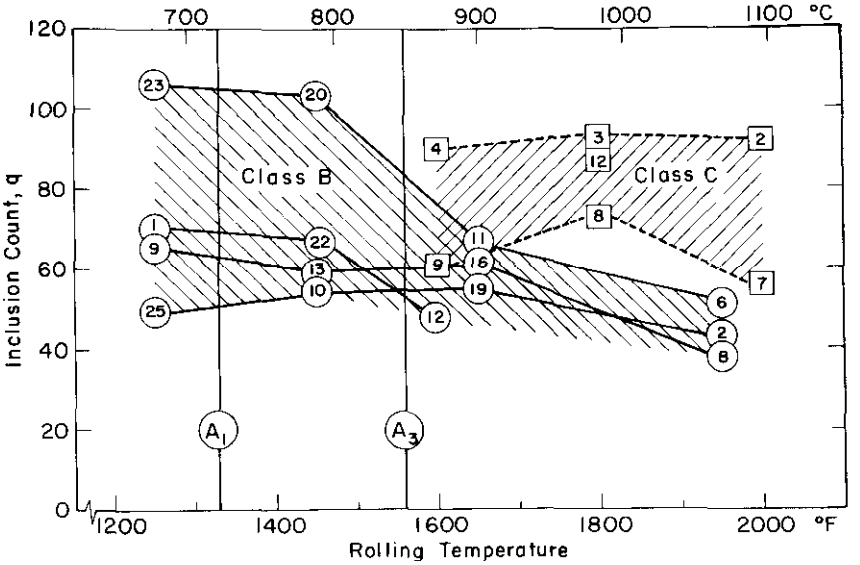

Fig. 3. Dependence of the Fibering Intensity Parameter, q, on Rolling History of Class B (O) and Class C (□) Plates. Numbers identify plates described in Table II. Points representing the same percent reduction are interconnected. Plates rolled according to non-isothermal practice (B-12, -22, -1; C-12) are represented by the temperature of the finishing pass. A_1 and A_3 are the lower and upper critical temperatures, respectively.

It is also known that heavier, more rapid and more nearly continuous deformation contributes to greater hot-work grain refinement.[22-25] One reason may simply be the reduced time for growth subsequent to new-grain formation. Within limits, a similar trend should follow from low deformation temperature. Considering the over-all cooling rate of plates rolled at 1450°F (see Appendix), the upper critical temperature (Ac 3) could not have been higher than about 1400°F. Therefore, a minimum austenite grain size, evident as a peak in ferrite grain-size number, would be a logical result of the heaviest reduction imposed at this temperature.

Rolling at 1250°F was probably not begun before at least partial transformation of the austenite, nor terminated before most of the transformation had occurred. With ferrite being formed from unworked austenite at 1250°F, the final grain size would necessarily be coarser than that from 1450°F finishing. Metallographically obvious strain markings and grain-shape distortion (Figure 4), together with higher hardness, reflected the incomplete recrystallization of ferrite after reduction at 1250°F. On the Rockwell-B scale, these plates were harder by 5 to 10 points than all others at comparable grain size (see Appendix Figure 3A).

The generally finer grain size of Class C plates, by about 0.5 ASTM units, is a natural reflection of the "fine-grain" practice by which the material is made, coupled with the fact that plates of this class were cooled and transformed before austenitizing and rolling. The grain-coarsening temperature for the steel under study was determined to be about 1725°F; details are given in the Appendix. However, there is no discontinuous change in grain size with rolling over a range including that temperature. Perhaps none should be expected, since tendency towards grain coarsening is modified by both prior treatment and deformation.[26] Therefore, any coarsening temperature measured in a "static" sense may have little significance in actual rolling.

Inclusion Character: The trend in B steel, of more elongation with heavier, lower-temperature reduction, is partly a consequence of the over-all shape change. Beyond this, it may also reflect the influence of

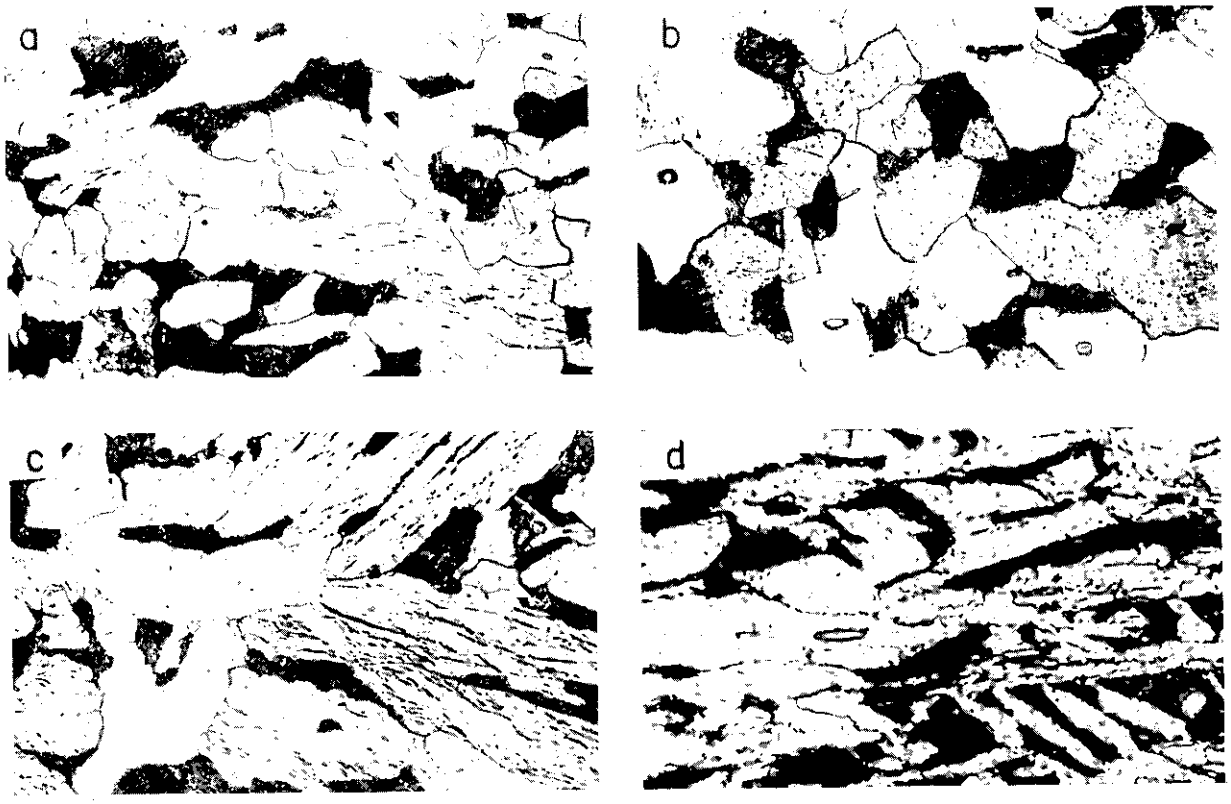

Fig. 4. Strain Markings and Grain-shape Distortion in Class B Plates Rolled at 1250 F (T-Z Plane). 2% Nital etch. 450 X

(a) B-1, 30% Non-isothermal. *(b) B-25, 15% Isothermal.*
(c) B-9, 30% Isothermal. *(d) B-23, 60% Isothermal.*

rolling pressure being increased with lower temperature and thus acting to elongate inclusions more, as discussed by Pickering.[27] Inclusions in C steel are generally longer than in B because silicates, which have high plasticity,[28] are more plentiful, and silicate and sulphide are agglomerated in a larger, duplex form.

Pearlite Morphology: Pearlite-patch size varied more or less as did ferrite grain size, although with much scatter in the measurements. The amount of pearlite ranged from 18 to 28 volume percent, but was not systematically related either to rolling history or subsequent heat treatment. Interlamellar spacing could not be correlated with rolling practice.

Crystallographic Texture: Various plates were examined, but only in B-23 (60 percent at 1250°F) was the preferred orientation sufficiently well developed to permit the plotting of a pole figure. Using a modification of the Schulz reflection technique,[29] the three mutually perpendicular surfaces of a 1/2 inch cube (oriented along R, T, and Z directions) were examined. The basic although diffuse texture was (001) [110], which has been found previously after rolling at temperatures as high as 1440°F.[30,31]

B. Properties and Behavior

Tensile Testing: Selected examples of test data are given in Figure 5. Plates B-2 and B-23 were chosen as they represented extremes in rolling history from the lightest high-temperature reduction (15 percent at 1950°F) to the heaviest low-temperature reduction (60 percent at 1250°F). As in past work,[6] the intersection of yield and fracture-stress curves defined a ductility-transition temperature, DT.

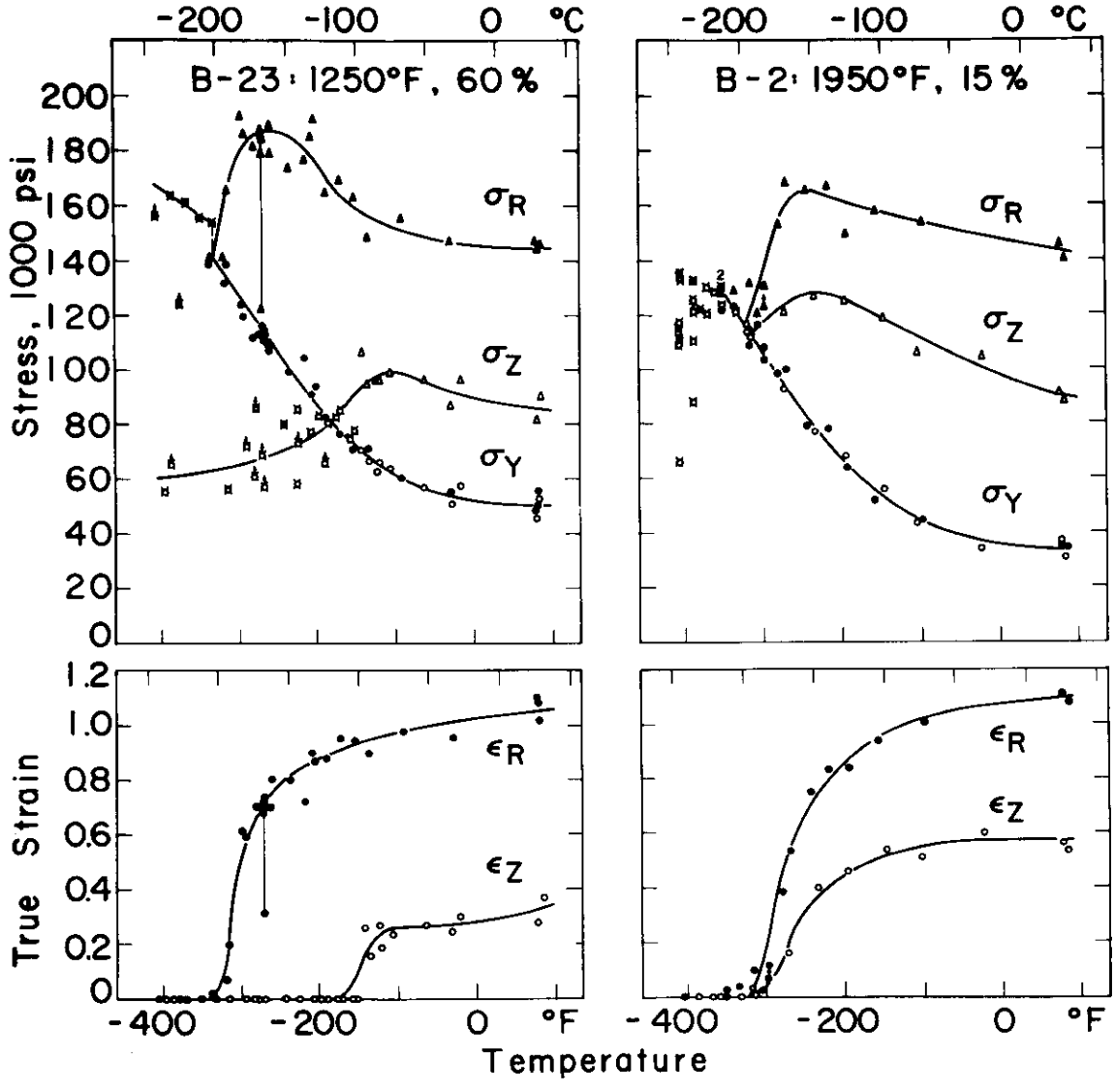

Fig. 5. Temperature Dependence of Tensile Yield Stress (σ_Y) True Fracture Stress (σ_R, σ_t) and Strain (ϵ_R, ϵ_Z) for Plates B-23 and B-2. Fracture in the absence of measurable plastic strain is indicated by ✖ or ⨳. Certain fractures located where gripping fixtures bore on the specimen have been treated by dividing load by minimum cross sectional area and plotting the result with an arrow pointing upward. For the example of fracture outside of the neck region, stress and strain have been computed with both actual fracture area and the minimum area in the neck; results are connected by a vertical tie-line.

Certain fracturing peculiarities were encountered, particularly in B-23. Below DT, fracture in the Z direction sometimes occurred at stresses substantially below the yield stresses; occasionally such fractures were found in other plates and in the R direction as well. In metallographic sections (Figure 6), the fractures are seen to have followed closely the direction of mechanical fibering. They were probably initiated at inclusions acting as internal notches, after which propagation followed at very low stress.

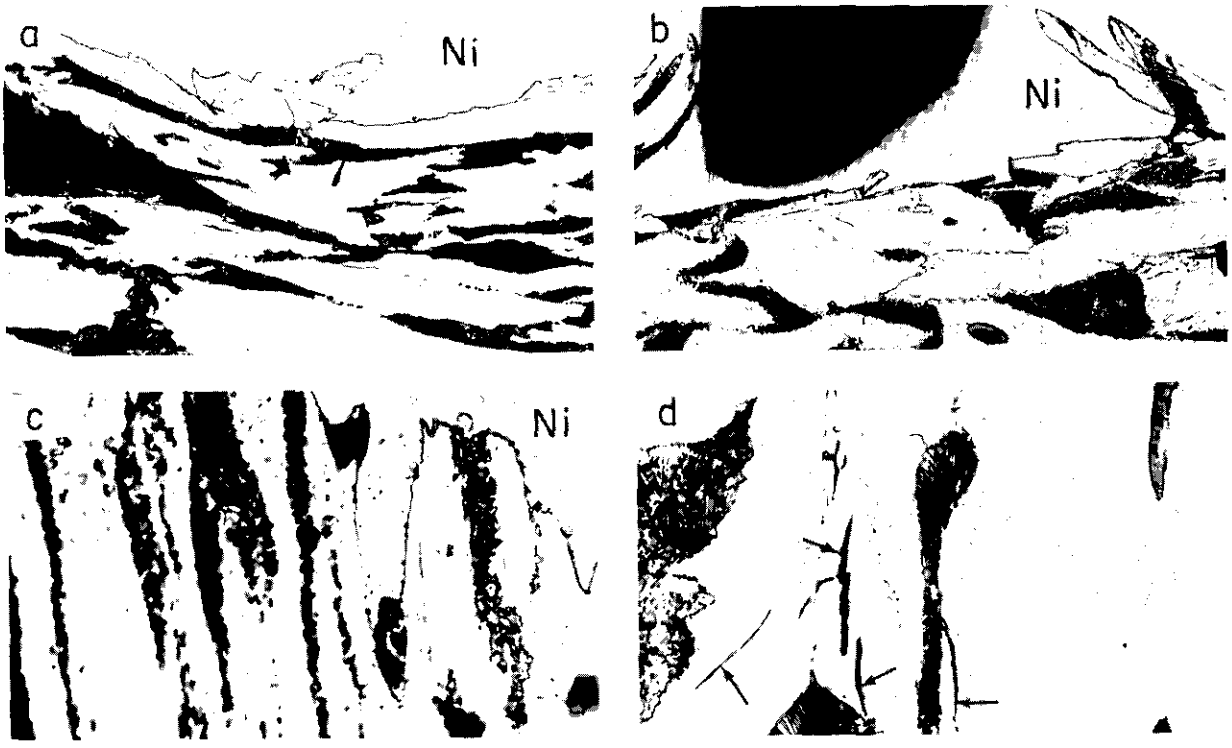

Fig. 6. Microsections (R-Z Plane) of Tensile Specimens from Plate B-23 Showing Fracture Surfaces (Ni-Plated) in Obvious Relation to Mechanical Fibering. Tensile axis vertical in all cases. 2% Nital etch.

(a,b) Fracture at stress below the yield level in a Z-direction specimen pulled at -396 F. 450X

(c) Rolling-plane delamination initiated at an inclusion in an R-Direction specimen pulled at -171 F. 900X

(d) Cleavage cracks (indicated by arrows) aligned along load axis in an R-direction specimen tested at -315 F. 900X

In one instance of an R-direction test on B-23, above the DT and near the peak of the fracture-stress curve, fracture took place well outside of the neck. While the stress at the actual site was only slightly above the lower yield, the value at the center of the neck was more nearly equal to the expected fracture stress. Also, under these general conditions, R-direction specimens occasionally failed by a combination of longitudinal splitting along the rolling plane through the neck (displaying a surface of "woody" appearance) and a normal crystalline-appearing separation at the ends of the split (Figure 7). Evidently, the transverse stress introduced with necking became as large as the prevailing Z-direction fracture strength, brought down to this low level by mechanical fibering, examples of longitudinal splitting are also shown in Figure 6; in Figure 6d, cleavage cracks are clearly aligned along the R direction.

Another observation was that of an elliptical cross section in R-direction tension specimens from plates rolled at 1250°F and 1450°F, the minor axis being aligned with the Z and the major axis with the T direction. The largest ratio of true strain in the Z direction to that in the T was about 1.75, independent of test temperature, and found in plate B-23. Such plastic anisotropy is a reflection of the crystallographic texture, previously noted as being strong enough after the 60 percent reduction at 1250°F to permit pole-figure description. Even though texture was too diffuse for diffraction analysis after 1450°F reduction, it was still evident in this

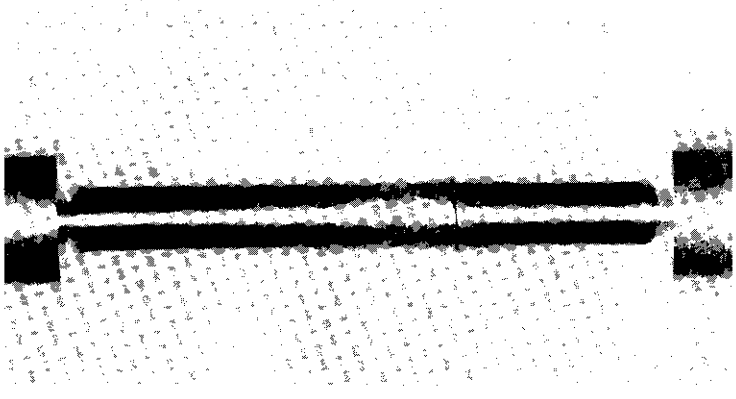

Fig. 7 (a). R-direction Specimen of Plate B-23 Pulled at -270 F (DT = -333 F) Which Fractured Outside the Neck.

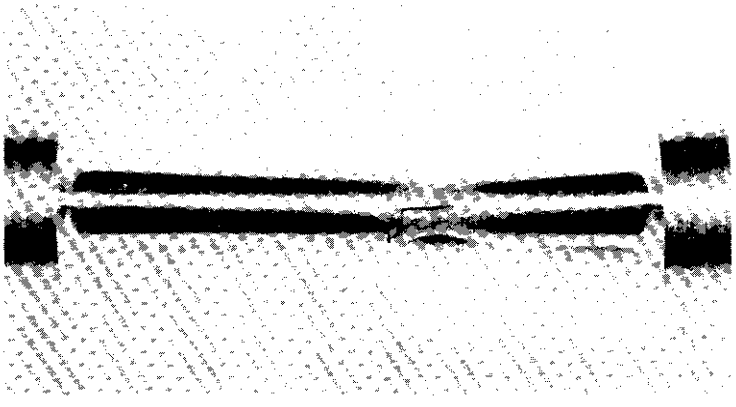

Fig. 7 (b). R-direction Specimen of Plate B-23 Pulled at -261 F (DT = -333 F) Which Failed by a Combination of Longitudinal Splitting Along the Rolling Plane Through the Neck and a Normal Crystalline Appearing Separation at the Ends of the Split.

departure from circular cross section. A basis can be found in recent calculations for expecting a plastic anisotropy with greater Z-direction strain as a consequence of the observed texture.[32] Also, from anisotropic plasticity theory, it can be argued that in plate B-23 the plane-strain yield stress at the root of a notch through the thickness direction (as in a conventional Charpy specimen) ought to be increased by about another 3-1/2 percent above the usual $(2/\sqrt{3})$ x (uniaxial yield stress) for an isotropic material.[32] An effect of this kind might properly be regarded as embrittling, although only mildly so.

All tensile ductility-transition temperatures are plotted against rolling temperature in Figure 8 (with tabulation in the Appendix). Only the Z-direction values, DT_Z, appear sensitive to rolling history, the level being increased sharply in the extreme case of plate B-23. Some of the reason is found in mechanical fibering (Figure 3), the more intense fibering acting to raise DT_Z. That more is involved is evident from specific comparisons, as between B-23 (q = 106) and B-20 (q = 103), which are similar in q but not in DT_Z, and between B-9 (q = 66) and B-20 (q = 103), in which case the higher DT_Z is found in B-9. Residual cold work must also be involved. It was most intense after the heaviest 1250°F reduction and correlates with the highest DT_Z for these conditions.

Various ratios of fracture stress and strain in R and Z directions may be used to demonstrate the marked fracturing anisotropy. Those formulated from true stress and strain at fracture in room-temperature tests were as revealing as any, and are plotted against q, with good correlation, in Figure 9. Figure 10 contains examples of ductile Z-direction fractures in which the separation around inclusions is clearly seen. Class-C anisotropy was consistently greater, which is to be understood against the background of duplex and more massive inclusions in this material. R-direction properties for both C and B stock were much the same; the difference grew out of the lower levels along the Z direction in Class C.

A further indication of residual cold work from 1250°F finishing was evident in the Petch-type plots of lower yield stress vs. (grain diameter)$^{-1/2}$.[33] Such plots are given for all B plates at selected test temperatures in Figure 11. A reasonable least-square fit can be made to the data, excluding those from the plates finished at 1250°F; σ_y is consistently higher in the latter four cases, which is interpretable as an increase in the friction stress, σ_i, from cold work. The increase in σ_i (or lower yield stress) above the trend-line levels is listed in Table IV for the 1250°F plates at the several test temperatures. The average increase is found to be larger the greater the amount of reduction imposed on the ferrite, assuming that the non-isothermal B-1 fits between B-25 and B-9.

Charpy Impact Testing: These results were much more influenced by reduction schedule (Figure 12). Trends were determined basically by ferrite grain size (Figure 2) and residual cold-work (Table IV). The inverse linear relationship between T_{V-15} and ASTM grain-size number is shown in Figure 13, where the slope for both Class B and C of -20°F (-11°C)/ASTM No. is in the usual range.[6,9]

Two extra-grain-size effects are immediately apparent in Figure 13: One is the roughly 40°F (22°C) displacement between Class B plates rolled at and above 1250°F (Figure 13a), which has its origin in residual cold work. The other is the 24°F (13°C) separation between the two as-rolled Class B and C trend lines (Figure 13d). From previous work, it should be expected

that at least part of this separation can be rationalized in terms of chemical-composition differences.[4] The most detailed study of transition

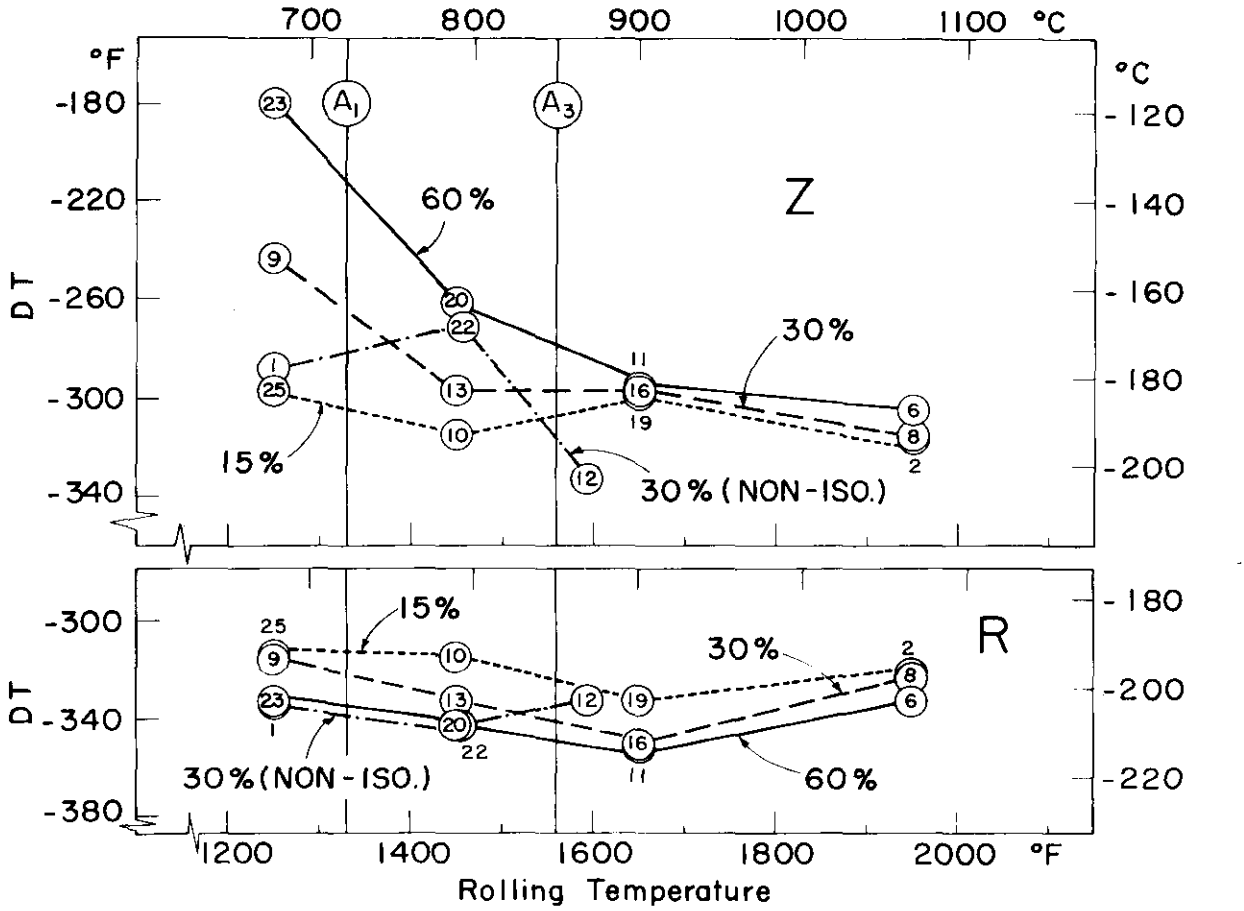

Fig. 8. Dependence of Tensile-Ductility Transition Temperature on Rolling History of Class B Plates. Numbers identify plates described in Table II. Points representing the same percent reduction are interconnected and labelled. Plates rolled according to non-isothermal practice (B-12, -22, -1) are represented by the temperature of the finishing pass. A_1 and A_3 are the lower and upper critical temperatures, respectively.

temperature in relation to composition is described in a recent report by Boulger and Hansen to the Ship Structure Committee.[9] With coefficients established in that work, by simple correlation analysis, a difference in T_{V-15} at constant grain-size can be calculated from the two analyses in Table I which is exactly the observed 24°F (13°C). However, by calculating with a formula generated in the same work through a more rigorous multiple correlation analysis, the difference is found to be only 5°F (3°C). The discrepancy might be understood on the basis of the uncertainty inherent in such work. Conversely, other factors may be involved which might be exploited, if they could be identified.

A third possible extra-grain-size effect would be that derived from microfissuring. Although a fairly wide variation in fracturing anisotropy

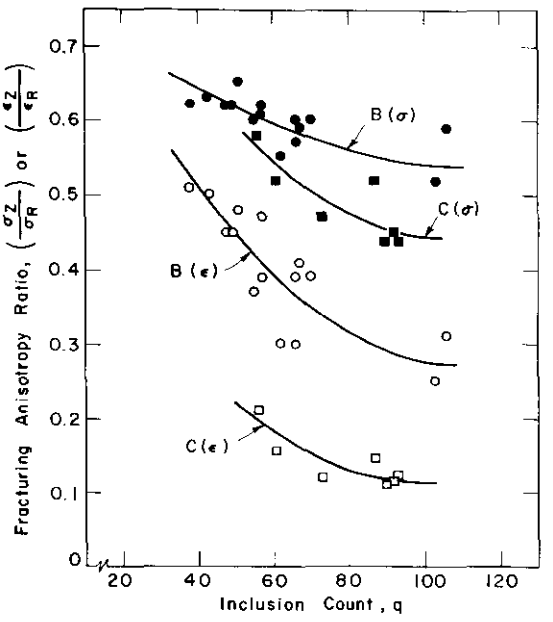

Fig. 9. Dependence of Room Temperature Fracture Anisotropy in As-Rolled Class B and Class C Plates on the Fibering Intensity Parameter, q.

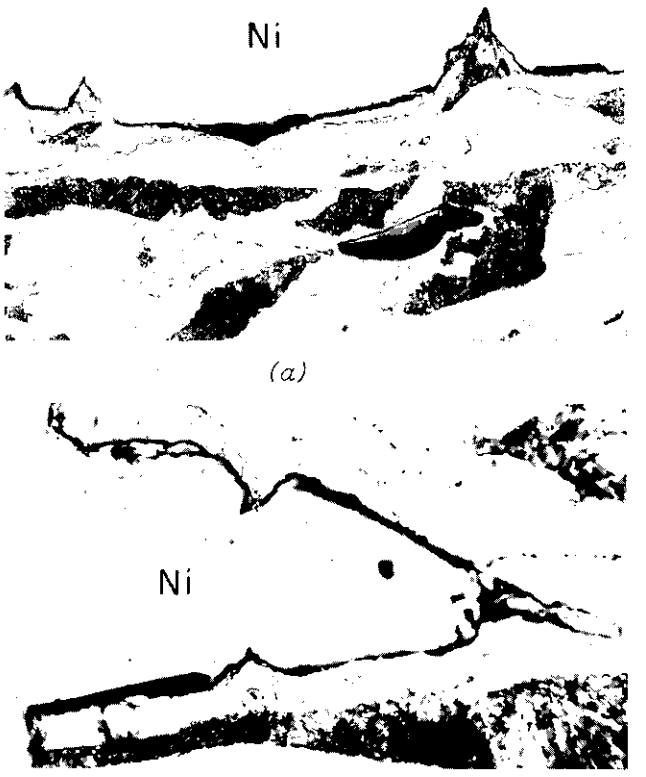

Fig. 10. Examples of Ductile Z-direction Fractures in Plate B-23 at -142 F (DT = -180 F), Showing Separation Around Inclusions. (a) 381 X (b) 881 X

TABLE IV. TEMPERATURE DEPENDENCE OF YIELD PARAMETERS.

Test Temperature °F	Class B Plates Rolled Above 1250°F		Class B Plates Rolled at 1250°F			
	Friction stress, σ_i (1000 psi)	Locking strength parameter k_y (1000 psi-mm$^{-1/2}$)	Increase in lower yield stress (or friction stress) from cold-work (1000 psi)			
			B-25	B-1	B-9	B-23
RT	14.05	4.42	5.5	6.5	5	18
-100	18.42	6.17	5	6	11	15
-145	36.10	4.44	6	7	12	15
-235	67.30	3.38	5	5.5	10.5	14
-280	88.60	2.70	3.5	6	13	15
-320	93.50	4.94	8	8.5	12.5	19
Average Value	-----	4.35	5.5	6.5	12	16

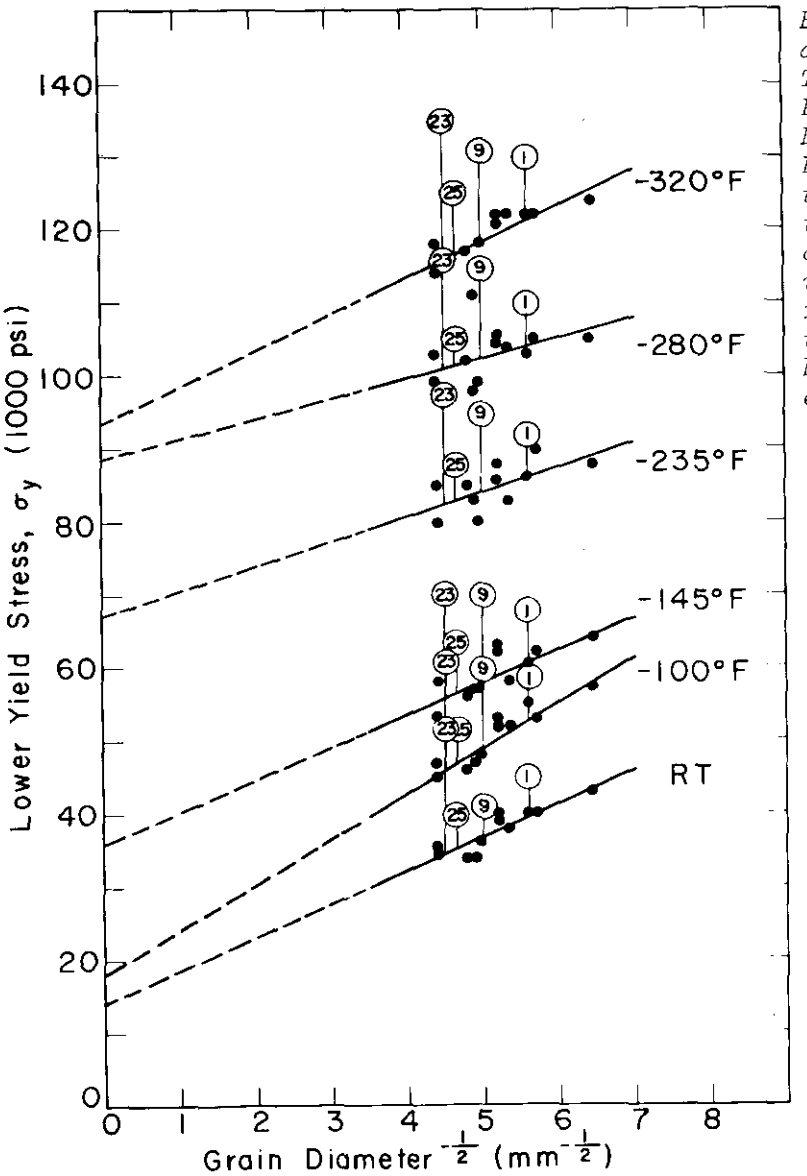

Fig. 11. Grain Size Dependence of Lower Yield Stress in Tension (σ_Y) for Class B Plates from Room Temperature to Liquid Nitrogen Temperature. Plotted values of σ_Y were taken at the selected temperatures from curves of the type drawn in Fig. 5. Points are identified only for the plates rolled at 1250 F (see Table II); these are joined by tie-lines but were not considered in establishing the main plots.

was established (Figure 9), it was unfortunate from the point of view of observing an effect that its contribution to $T_{\nu-15}$ was too subtle to appear against the background of other structural contributions.

No correlation could be made between the Charpy-test results and the volume fraction, patch size, or interlamellar spacing of pearlite.

All heat treatments were evaluated by impact-testing, and fall generally into three categories:

(1) The first involves the various annealing and homogenizing treatments (Table III), performed only on Class B plates. Results in this category are summarized in Figure 13b, where it is clear that all changes in $T_{\nu-15}$ were consistent with changes in ferrite grain size.

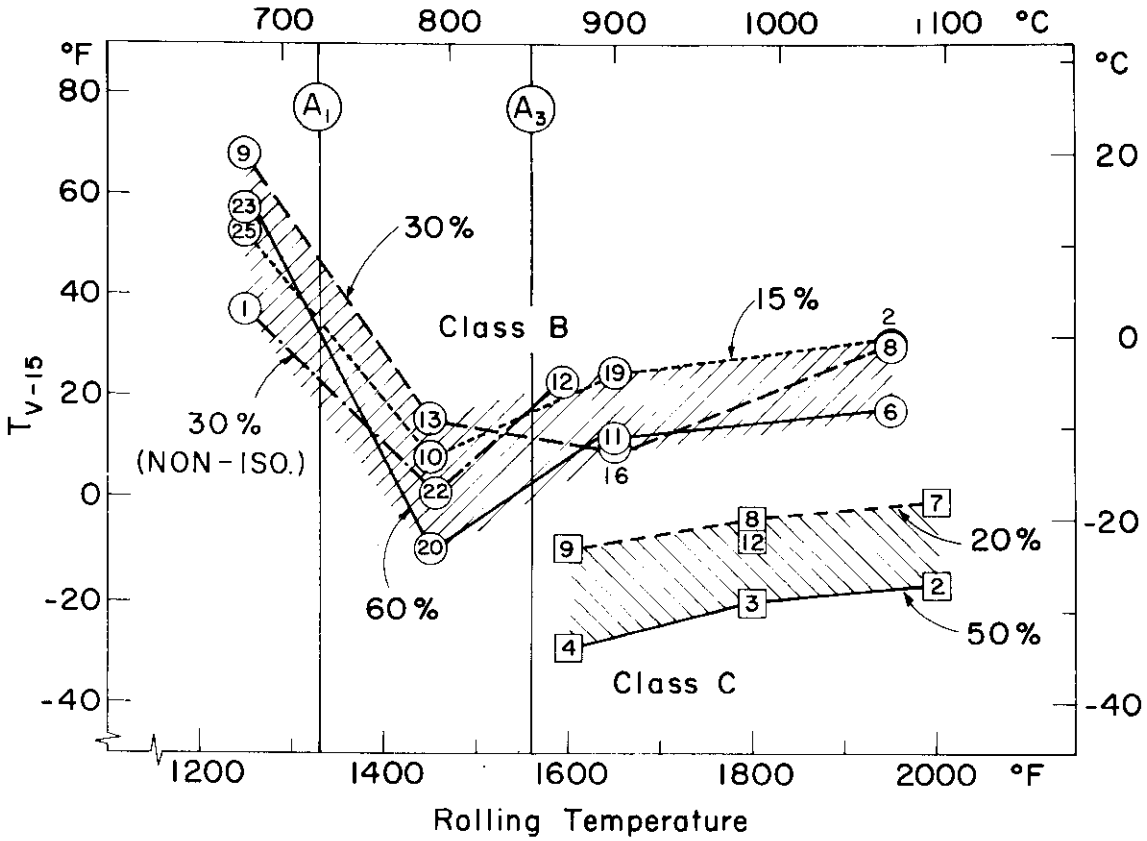

Fig. 12. Dependence of 15 ft. -lb. Charpy-V Transition Temperature (T_{v-15}) on Rolling History of Class B (O) and Class C (□) Plates. Numbers identify plates described in Table II. Points representing the same percent reduction are interconnected and labelled. Plates rolled according to non-isothermal practice (B-12, -22, -1; C-12) are represented by the temperature of the finishing pass. A_1 and A_3 are the lower and upper critical temperatures, respectively.

(2) The second relates to normalizing, which introduced varying amounts of Widmanstätten structure (from 10 to 35 percent) into Class B plates while eliminating differences between as-rolled microstructures. In the presence of this structure, ASTM No. was based on the mean intercept from a traverse that excluded Widmanstätten areas. As shown in Figure 13a, the T_{V-15} of plates rolled at 1450°F and above (B-2, 8, 10, 16, and 20) were raised, while those of plates rolled at 1250°F (B-9 and 25) were lowered. The final trend line approached from both directions is about 11°F (6°C) higher than that for the as-rolled condition. Plate 8Haa fits in with the others, even though given an homogenizing anneal before normalizing. The extra-grain-size effect implied in such results is probably no more than an apparent one, however; the reason is that Widmanstätten areas are normally several times larger than the ferrite grains and, owing to similarity of orientation among the constituent plates or grains, may have much the character of individual ferrite grains during deformation and fracture. An example in Figure 14 of a twin continuing across several ferrite regions illustrates this possibility. Accordingly,

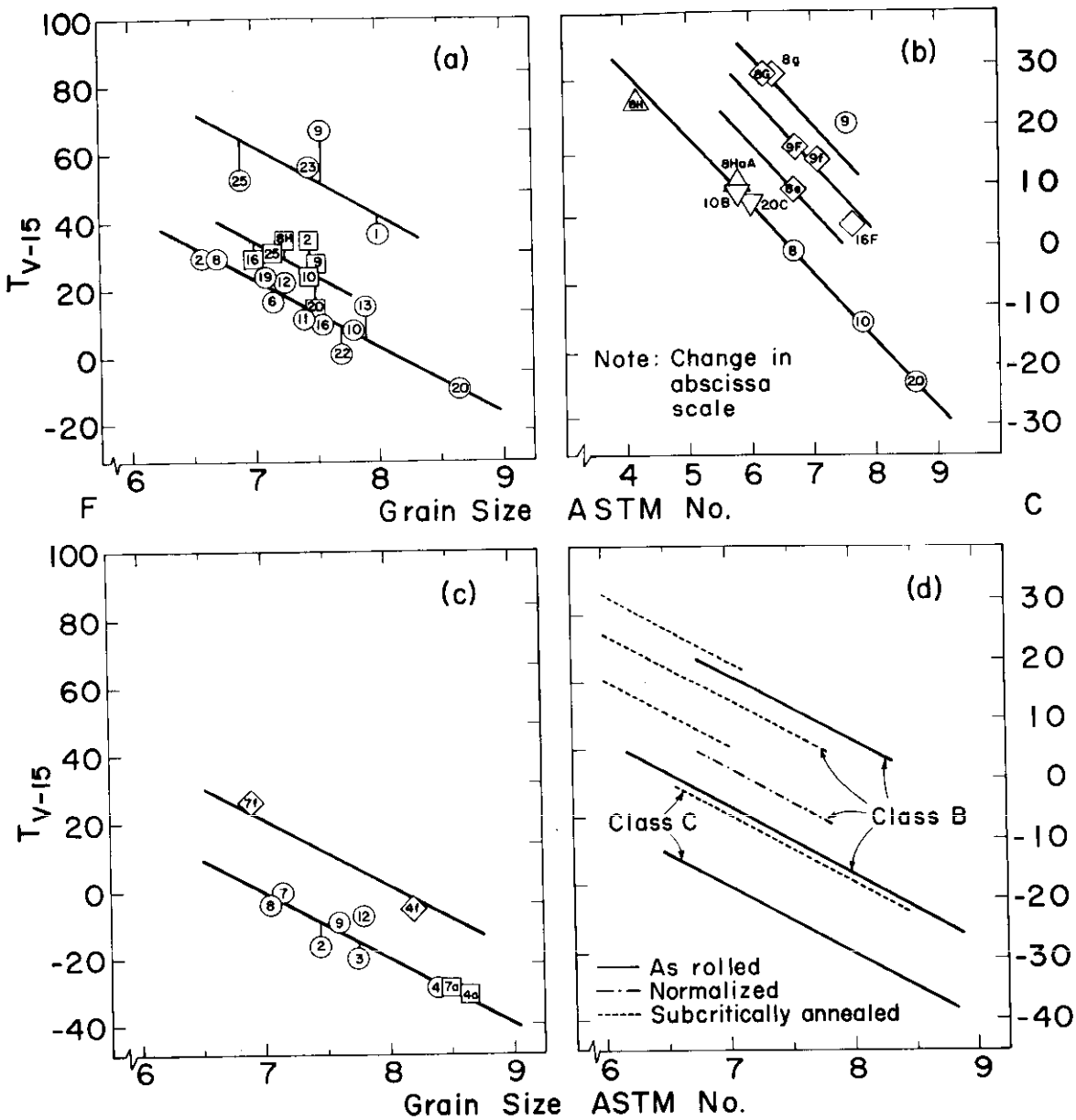

Fig. 13. Grain Size Dependence of 15 ft.-lb. Charpy-V Transition Temperature (T_{v-15}) for As-Rolled and Heat-Treated Plates.

(a) Class B, as-rolled (O) and normalized (□).
(b) Class B, annealed (▽), homogenized (△) and subcritically annealed (◇); as-rolled (O) included for comparison.
(c) Class C, as-rolled (O), normalized (□) and subcritically annealed (◇).
(d) Summary of all trends.

Numbers and letters identify plates and heat-treatments described in Tables II and III, respectively.

Fig. 14 (a). Twin Continuing Across Several Adjacent Ferrite Regions of a Widmanstätten Colony, Suggesting Similarity of Orientation Among the Regions. Z-direction specimen from plate B-2 pulled at -272 F. 2% Nital etch. 450X

Fig. 14 (b). View of Unusually Well Developed Widmanstätten Pattern in Coarse Pearlite of Plate 8H, Formed During the Eutectoid Transformation on Cooling After Homogenization. 2% Nital etch. 90 X

Widmanstätten structure might be regarded as equivalent to coarse ferrite grains, so that the usual intercept method of ferrite grain-size determination could lead to an underestimation of effective grain size. Such an effect after air-cooling and the introduction of Widmanstätten structure has been reported earlier, but attributed to substructural changes not evident in the gross microstructure.[5] The normalizing of Class C plates resulted in no Widmanstätten structure, and the T_{V-15} in Figure 13c lay on the as-rolled trend line, changed (lowered) only by grain refinement.

(3) The third category represents the subcritical treatments, planned initially to isolate temperature and cooling-rate effects in low-temperature finishing. From the various treatments (Table III), slight decreases in both Rockwell-B hardness (about 5 points on the average) and lower yield point (about 2500 psi on the average) were noted, but the yield-point drop and Lüders strain were unaffected.

The T_{V-15} of plates B-8 (8e, 9g, 8G) and B-16 (16F) were raised, while that of B-9 (9f, 9F) was lowered. The results are given in Figure 13b with trend lines drawn to suggest that the embrittlement (relative to the as-rolled Class-B trend) is dependent primarily upon duration of annealing and insensitive to cooling conditions. A similar T_{V-15} elevation for C steel is shown in Figure 13c. With such treatments, it was also noted that the impact-

energy vs. test-temperature curves became more steep and that the maximum amount of energy absorbed was increased by as much as a factor of 2 in some instances. The data are summarized in Table V.

Stout and McGeady[34] also observed embrittlement in a 0.25 percent C Si-killed steel after holding at 1200°F for 1 hour and air cooling; aging was suggested in explanation of that finding. It is difficult for two reasons to understand how the subcritical embrittlement can be interpreted relative to aging: The degree of embrittlement is strongly dependent upon time at temperature, yet dislocation atmospheres ought not to be stable above about 800°F.[35] The insensitivity of tensile yield behavior to time at 1250°F or to cooling conditions reinforces this position. Thus changes in the ferrite *per se* may not be responsible. In that vein, there was no effect upon the T_{V-20} transition temperature of a 0.01 percent C iron after holding at 1250°F for 15 minutes.[36] Moreover, fracture in Charpy specimens of the present work, heated at 1250°F and broken near the transition temperature, was mainly transgranular cleavage which rules against any grain-boundary embrittlement acting to lower the notch toughness.

The obvious change in microstructure with 1250°F heating was spheroidization. Although that development is usually associated with the toughening of medium and high-carbon steel, there is at least one observation by Rinebolt[37]

TABLE V. RESULTS OF SUBCRITICAL HEAT TREATMENTS.

Plate No. (Table III)	Heat Treatment		Spheroidization of Cementite, %	ΔT_{V-15}*, °F	Maximum Energy Absorbed ft-lbs
	Duration, hrs.	Cooling			
B-8	as-rolled		0	--	107
B-8e	1	air	50	18	> 140
B-8g	10	air	100	45	200
B-8G	10	furnace	100	43	> 190
B-9	as-rolled		0	--	> 90
B-9f	2	air	80	36**	> 130
B-9F	2	furnace	80	32**	108
B-16	as-rolled		0	--	102
B-16F	2	furnace	80	27	176
C-4	as-rolled		0	--	128
C-4f	2	air	50	18	> 180
C-7	as-rolled		0	--	127
C-7f	2	air	50	25	152

*In relation to the trend line for the as-rolled plates.
**Taken relative to the as-rolled trend line for plates rolled at 1450 F and above.

of the opposite effect in a 0.3 percent C steel. Upon plotting ΔT_{V-15} against percent spheroidization, from Table V, the result is a reasonable straight line which at least suggests a physical relationship (Figure 15). Some basis for such a relationship might be found in alterations at the ferrite-pearlite interface. With spheroidization in these low-carbon steels the ferrite-pearlite interface may become less effective in its ability to arrest a cleavage crack. Representative microsections are shown in Figure 16. In Figure 16a, a cleavage crack (Ni filled in plating) has travelled across a considerable region of spheroidized cementite. In Figure 16b, cracks are

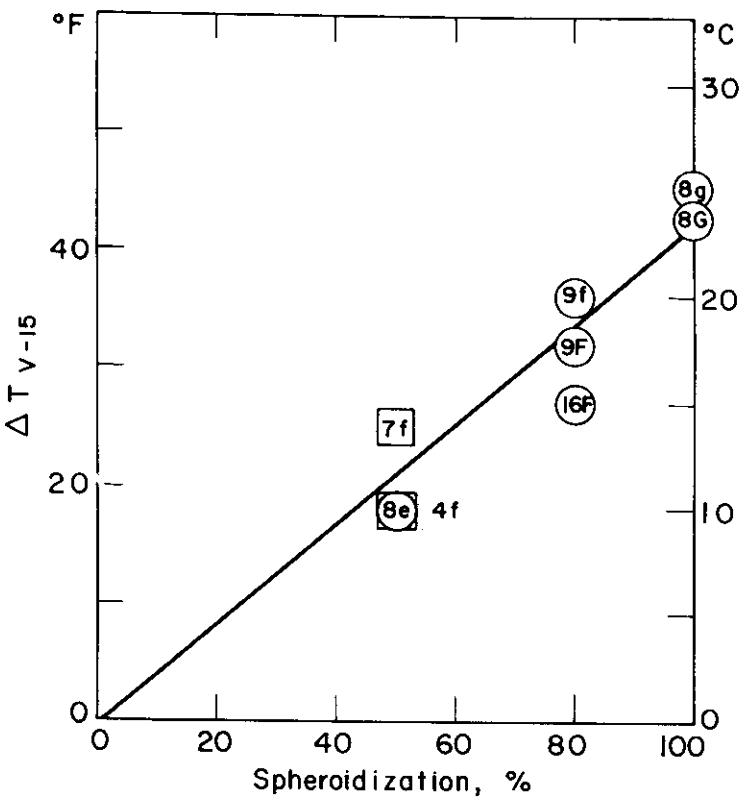

Fig. 15. Rise in T_{V-15} as a Function of Percent Spheroidization During Subcritical Annealing of Class B (O) and Class C (□) Plates.

seen in both pearlite and ferrite, but there is a strong suggestion here of blunting and deflection at the pearlite-ferrite interface.

Whatever the full reason for the embrittlement, it is equivalent in its effect to a decrease in the ASTM grain-size number of as-rolled ferrite by as much as 2 units, this being roughly the ratio of the maximum ΔT_{V-15} in Figure 15 to the -20°F/ASTM No. slope of the trend lines. Although the result of spheroidization might be regarded as an increase in effective mean-free crack path, there are still no grounds for imagining that change in carbide morphology, even to the point of its complete elimination from the microstructure, could account for such a large increase. The suggestion being made is only qualitative at best. Other support for it does come from the altered form of the impact-energy vs. temperature curve; that after 1250°F heating is more nearly characteristic of ferrite alone.[38]

A few results of tests on Charpy specimens taken parallel to the transverse direction (notch still along the z direction) are summarized in

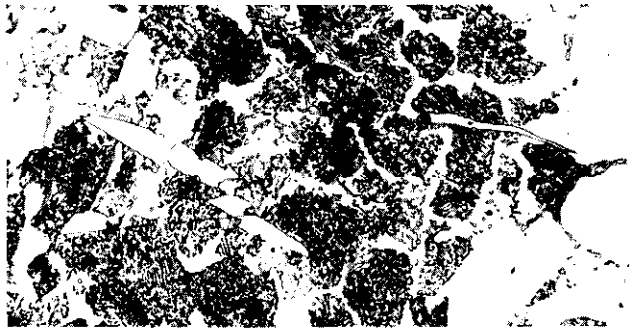

(a) Propagation of a cleavage crack (Ni filled in plating) across a considerable region of spheroidized cementite in a Charpy specimen from plate B-16F which absorbed 25 ft. - lb. at 50 F (T_{v-15} = 37 F). Large amount of cementite seen here (R-T plane) is a consequence of banding. 450 X

(b) Cleavage cracks in pearlite and ferrite blunted or deflected at the pearlite-ferrite interface. Z-direction specimen from plate B-2 pulled at -272 F. 950 X

Fig. 16 (a) and (b). Representative Microsections Comparing Cleavage Propagation Through Spheroidized Cementite and Pearlite. 2% Nital etch.

Figure 17. The greater anisotropy before compared to after heat treatment is to be expected in view of the reduced fibering intensity (lower q), chemical heterogeneity, etc. resulting from the treatments.

If over-all results are examined in relation to the 50 percent fibrous transition temperature, the outcome is much the same. The slope of $T_{v-50\%}$ vs. grain-size number was somewhat higher, being about -27°F (15°C)/ASTM No.

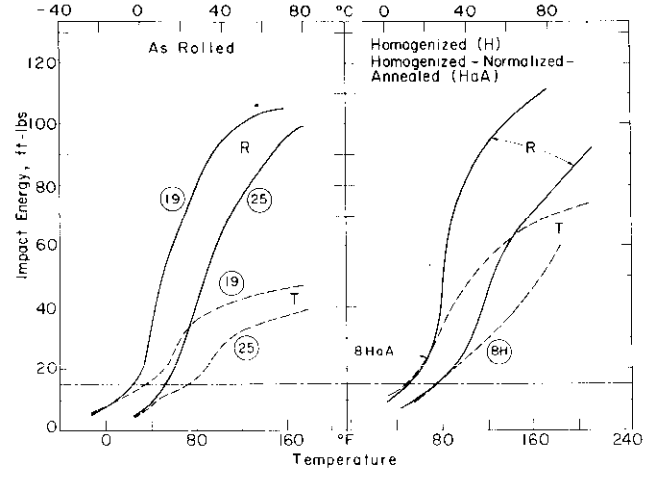

Fig. 17. Effect of Homogenization on the Orientation Dependence (R vs. T) of Charpy Impact Energy Absorbed as a Function of Temperature for Class B Plates. Transition curves of as-rolled plates 19 and 25 on the left are compared with those of homogenized (8H) and homogenized-normalized-annealed (8HaA) plates on the right. Numbers and letters identify plates and heat-treatments described in Tables II and III, respectively.

for both Class B and C. All $T_{V-50\%}$ and T_{V-15} data are correlated in Figure 18 with tabulation in the Appendix. The major difference in results with the two criteria was that no distinction could be made between Class B and C on the basis of $T_{V-50\%}$. Accordingly, the B-C separation in Figure 18 is the same as that in Figure 13.

C. Fracture Observations

Microcracks: Metallographic studies of fracture were made on Charpy and tensile specimens tested at temperatures somewhat above and below the T_{V-15} or DT. In general, the cleavage fracture path for as-rolled as well as heat-treated plates was transgranular without preference for ferrite, pearlite, or Widmanstätten areas (Figure 19). An infrequent example of intercrystalline fracture is shown in Figure 19c.

It has recently been suggested that microcrack initiation by the cracking of grain-boundary carbide films may be important in the low-temperature brittle behavior of mild steel.[39] However, in the many microsections of the present work prepared from both as-rolled and heat-treated (including furnace-cooled) materials, no examples of these films could be found.

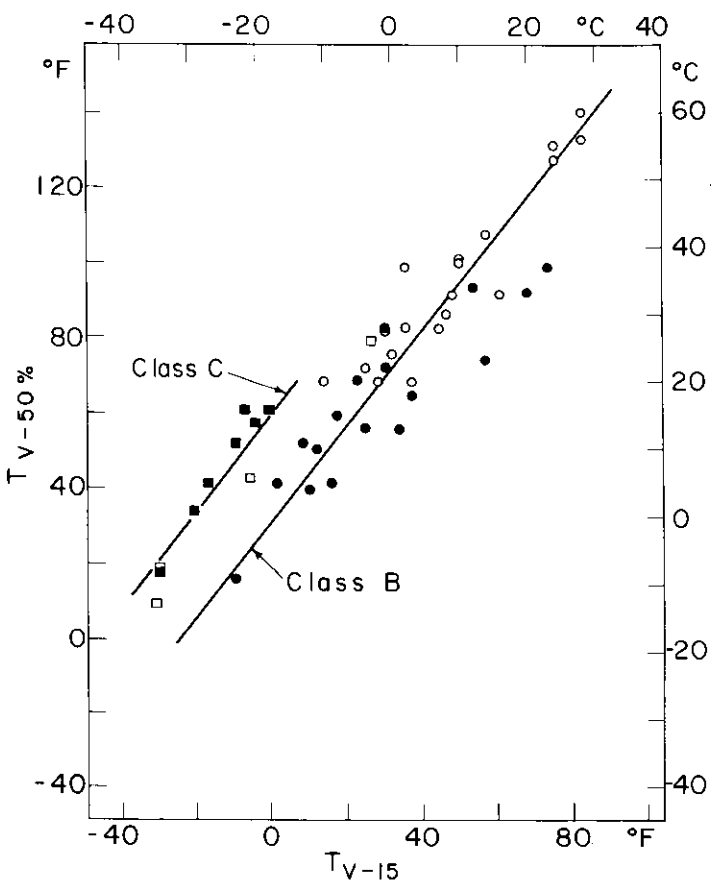

Fig. 18. Correlation Between $T_{v-50\%}$ and T_{v-15} for all As-Rolled and Heat-treated Class B (●, ○) and Class C (■, □) Plates.

(a) Cleavage initiation under the notch-root of Charpy specimen from plate B-2a, which absorbed 10 ft.-lbs. at 23 F (T_{v-15} = 36 F).

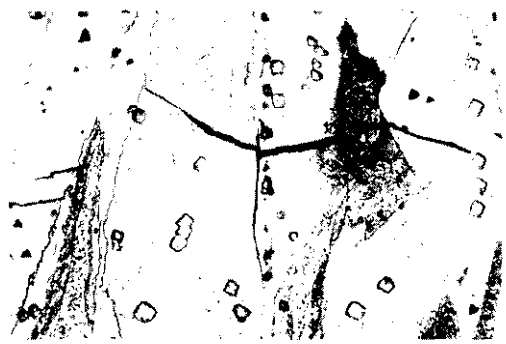

(b) Microcrack: etch-pit relationships confirm that ferrite cleavage occurs on {001} planes. R-specimen form plate B-23 pulled at -315 F.

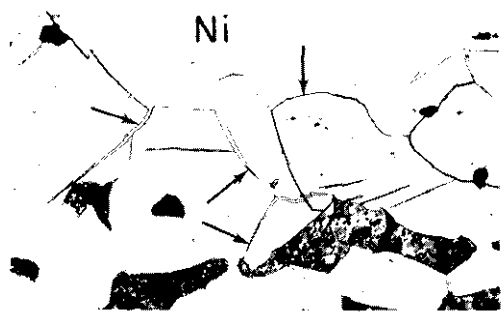

(c) Examples of intercrystalline fracture (indicated by arrows) in Z-direction specimen from plate B-2 pulled at -272 F (DT = 315 F).

Fig. 19 (a), (b), and (c). Examples of Fracture in Charpy and Tensile Specimens Tested Near the T_{v-15} or DT. 2% Nital etch. 450X

Electron Fractography: Examinations were made on the fracture surfaces of tensile specimens from plates B-2, B-20, and B-23 (Table II) taken along both R and Z directions and broken at temperatures from -63°F (-53°C) to -405°F (-243°C). Other studies were made on the delaminations, or rolling-plane splits, in R-direction specimens of plate B-23 (Figure 7); although surfaces of such orientation would be expected to yield the more detailed information on fiber structure, they seem not to have been investigated in work to date.

On all fracture surfaces, irrespective of macroscopic appearance, there were clear indications of cleavage and shear. The former is identified in Figures 20a and b by the usual "river markings" and the "tongues" formed through intersections of cleavage cracks and twins; the latter is represented in Figure 20c by the parabolic markings developed at inclusion sites. Although the amount of shear became less with falling test temperature, some was always found, even at the lowest temperature. A third type of fracture is shown in Figure 20d. It was observed with the least frequency and is

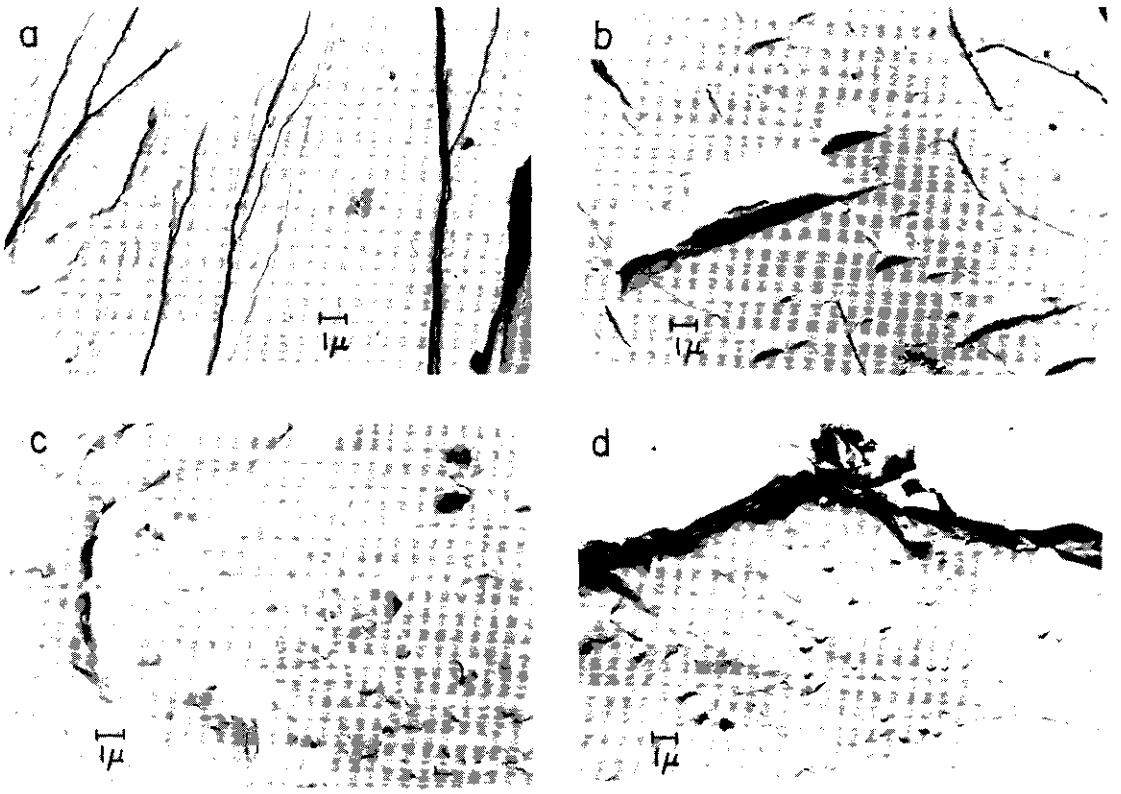

Fig. 20. Examples of Cleavage (a,b), Shear (c), and Intercrystalline (d) Fracture in Electron Micrographs.

(a,c) Delamination surface in an R-direction specimen of plate B-23 pulled at -272 F (DT = -333 F).

(b) Fracture surface of a Z-direction specimen of plate B-23 pulled at -396 F (DT = -180 F).

(d) Fracture surface of an R-direction specimen of plate B-2 pulled at -405 F (DT = -342 F)

characterized by a smooth, wavy surface free of "river" and "dimple" markings but containing inclusions; it might be classed as intergranular, resembling as it does the fracture from intergranular stress-corrosion[40] or that found in oxygen-embrittled iron.[41]

A number of observations were made of inclusions on fracture surfaces. They occurred with the lowest frequency among the obvious examples of cleavage. The greatest concentration of inclusions appeared on the delamination surface in R specimens of plate B-23, as brought out by selected illustrations in Figure 21. Since this was also the rolling plane, the high density and alignment can generally be understood. Because of cleavage steps observed in adjoining areas, Figure 21a is identified as cleavage. The alignment, presumably in the rolling direction, is most clear in Figure 21a with the particles in view being well flattened and apparently broken up into discs of 1μ or less in diameter by the heavy, low-temperature reduction. With reference to Figure 20d, the other examples in Figure 21 might be classed as intergranular. In Figure 21d, the local density is extraordinarily high; perhaps it reflects an accumulation of sulphide inclusions from interdendritic segregation.[42,43]

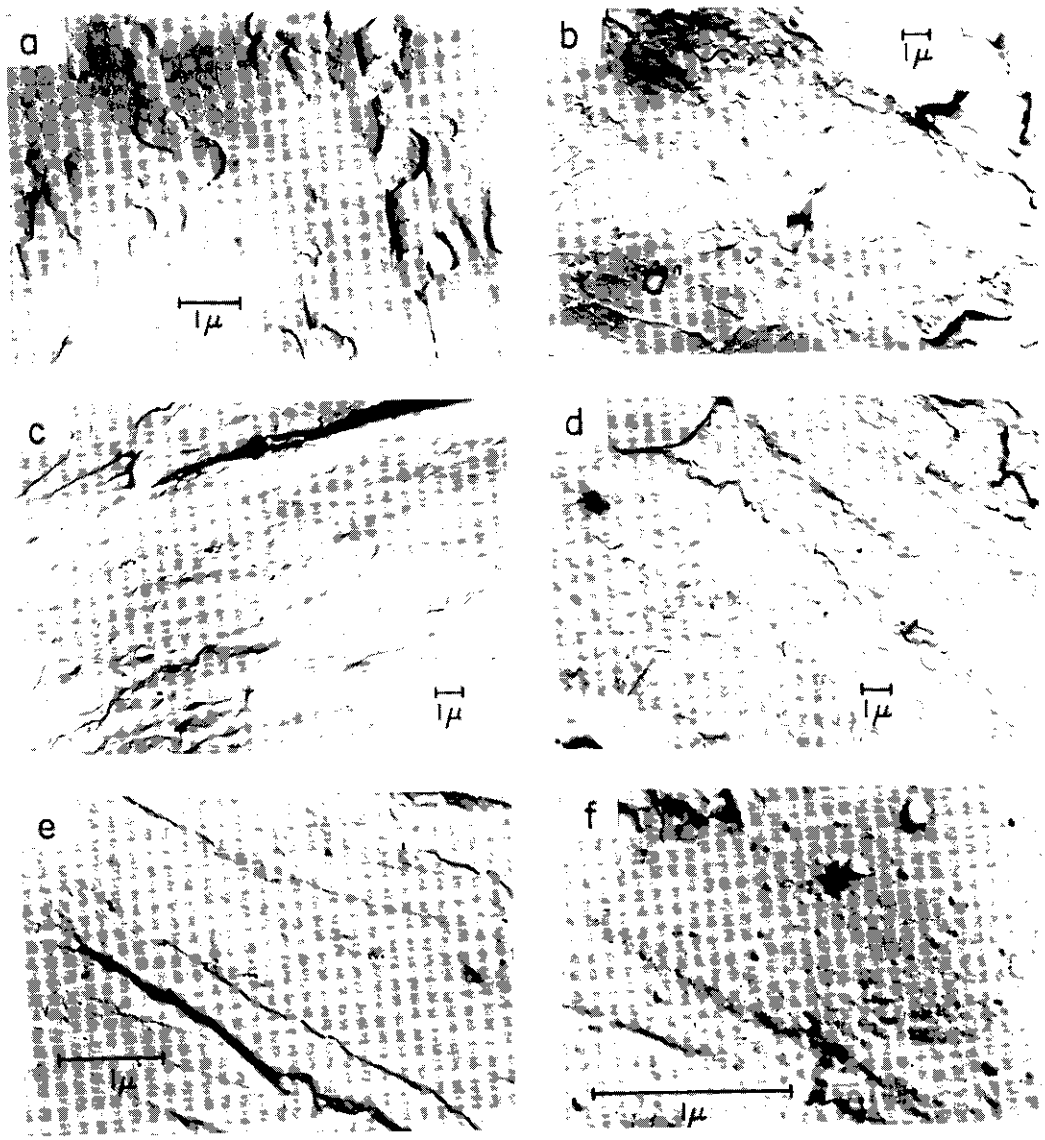

Fig. 21. Electron Micrographs of Inclusions in the Rolling-Plane Delamination Surface of Fracture in R-direction Specimens of Plate B-23 Pulled at -272 F (a to d) and at -261 F (e,f). (DT = -333 F) (a,e,f) : Cleavage. (b,c,d) : Intergranular

Even though the regions of structure shown in Figures 21a to d are only limited in extent, the understanding of many more macroscopic observations is improved by having noted them. Such aggregations of particles would contribute to the "woody" appearance of separations along the rolling plane. They could be responsible for initiation of below-yield fracture (especially in the Z direction) and delamination, and for tensile fracturing anisotropy in general, which is known to be related to mechanical fibering.[6,8] They may also correlate with the microfissures of about 5μ length and 2μ spacing observed in earlier work near the notch root of a Charpy specimen broken with only 6 foot-pounds energy absorption.[6] Further (and more typical) views of inclusions on cleavage surfaces, still in the rolling-plane delamination, are shown in Figures 21e and f at higher magnification. Here,

inclusions are more randomly distributed; as the size is reduced, towards about 0.1μ, they become more nearly spherical as well.

DISCUSSION

Observations have been made on several elements of structure as they relate to the ductile-brittle transition in ship-hull steels. Ferrite grain size proved to be by far the most significant, which confirms what is known from long experience, and it was shown once again that the T_{V-15} transition temperature is lowered by about 20°F (11°C) for each unit of increase in ASTM grain-size number. There can be little doubt that the structural route to low transition temperature lies along a trend line of the kind drawn in Figure 13. At the same time, the problems in attempting to follow such a route, within the framework of conventional practice, have been indicated.

In B steel, the result of more-or-less conventional finishing was ASTM 7.10 in B-12 (Figure 2). The smallest size was only ASTM 8.65 in B-20, produced by the unconventional 60 percent isothermal reduction at 1450°F. The grain size in other plates rolled at 1450°F was generally the next smallest, by about 1 ASTM unit (B-13, B-10, and B-22); of these plates, the Royal Netherlands practice was most closely simulated in B-22. Thus relatively little has been done to improve on established controlled-rolling practice for ferrite grain-size refinement. Similar findings were made in C-steel plates. The smallest grain size now was ASTM 8.3 in C-4, reduced 50 percent isothermally at 1600°F. The result of a more nearly standard practice was ASTM 7.7 in C-12.

Procedures to follow in moving still further down the T_{V-15} vs. ASTM No. trend line can be imagined, suggested, and even cited from experience. However, all would involve operational problems, difficult if not impossible to solve in current practice.

Small ferrite grain size is to be expected from austenite that is fine-grained prior to transformation.[22,23] Therefore, the need is to minimize pre-transformation austenite grain size. This can be done, in principle at least, by restricting austenite grain growth before reduction begins; some obvious possibilities are to introduce grain-refining agents in steel-making so as to elevate coarsening temperature,[44,45] or to cool and transform before reheating and rolling rapidly at the lowest possible temperature above the critical range. It can also be done by ensuring a maximum density of nucleation sites for austenite recrystallization during hot-working; now, the emphasis could be placed on heavy reduction to increase the ratio of grain-boundary area to grain volume[23,24] or on included particles which act as intragranular nucleation centers.[23,46] Still other possibilities relate to cooling-rate control, to minimize time for austenite grain growth in the interval between reduction and transformation, and to accelerate transformation; response to efforts in this direction should be improved in thinner plates.

Apropos to the last point, Stout and co-workers[47] found significant improvement in the notch toughness of pressure-vessel steels if, instead of normalizing, cooling from the austenitizing temperature was accomplished by spray-quenching; the effect was reported to result from ferrite grain refinement, although no quantitative comparison of grain sizes was established. As a further illustration, a ferrite grain size as small as ASTM 11 has been obtained in AISI 1020 Si-Al-killed steel bars by cooling from the

austenitizing temperature in air (to 1300°F), followed by lead (at 1100°F), and finally with a water-quench.[4] More pertinent to the entire last paragraph, the results of recently reported experiments[48] on medium-carbon steels demonstrate how extraordinarily small ferrite grain size may become under some conditions: The work involved heavy reduction at a temperature just above the upper critical and holding briefly for recrystallization before final cooling and transformation. In one example, an Al-killed 0.4 percent C steel plate 0.11 inch thick was reduced about 73 percent (to 0.03 inch) in one pass at 1500°F, held at this temperature for 10 seconds and air-cooled, to acquire a grain size of ASTM 14.

The development of the smallest grain size of ASTM 8.65 in plate B-20 of the present work is at least consistent with that pattern. The 60 percent reduction at 1450°F was probably completed above but near the upper critical temperature. It might be wondered if any more refinement could have been obtained by faster reduction, shortened cooling time, and smaller prior austenite grain size. In comparison of as-rolled grain sizes, those of Class C were generally the smaller for reason of the fine-grain practice and the fact that C-steel plates were cooled and reheated through the critical range before rolling. Nevertheless, improvement measured by the difference between ferrite grain size produced according to conventional and controlled practices was about the same for both B and C, cf. Figures 2 and 13. Apparently this has not been the finding of others who have reported greater improvement in semi-killed material.[11]

Normalizing after rolling is a possibility for further grain-size refinement, although its effect on B steel was clearly adverse, acting to coarsen grains developed in low-temperature (1450°F) reduction. In addition, it produced the general elevation of trend line by allowing Widmanstätten structure to form (Figure 13a). There was no grain coarsening in C-steel, the holding temperature being below that level, but neither was there any significant refinement either after the low-temperature finishing. Instead, the comparison for C-steel suggests an equivalence, in capacity for grain refinement, between normalizing and low finishing temperatures.

After exhausting the possibility of toughening by grain-size reduction, at least one alternative remains. With reference to Figure 13, this is a vertical descent exploiting any available extra-grain-size effects. The largest of these are generally chemical in origin, as reflected in the separation between as-rolled B and C trend lines (Figure 13d) and in the various transition-temperature formulas with their terms for calculating the contributions of individual components.[7,9] However, such effects may also be related to rolling practice.

Mechanical fibering has been identified as the source of one in the non-chemical category. Since this is a common development in wrought materials, its contribution ought to be expected more generally than not. The amount by which transition temperature may be lowered has been evaluated according to different criteria and found, in the case of T_{V-15}, to be of nearly the same magnitude as the experimental uncertainty of measurement.[6] Therefore, with the range of rolling conditions involved in these experiments, it is perhaps not surprising that the specific effect was not isolated, although the prerequisite structure was present and studied in some detail. Still another such effect may be based on the preferred crystallographic orientation found after rolling as high as 1450°F, but much more in evidence after the 1250°F reductions; both the mechanical and

crystallographic anisotropy can be identified broadly with texture. In principle, the latter can contribute as either a negative or positive extra-grain-size effect, depending upon details of texture. In hot-rolled steels, it is probably subtle in the extreme, although in inherently more anisotropic materials the contribution may be large.[32] Residual cold work underlies the remaining effect, which is negative in character and must function as a structural, if not practical, deterrent to finishing too low in temperature. The amount of embrittlement, rated as an increase in T_{V-15} for fixed grain size, can be rationalized with available theory, as it has been applied before to the similar problem of irradiation embrittlement (see Appendix).

SUMMARY AND CONCLUSIONS

The influence of hot-rolling practice on the structure and mechanical properties of ABS Class B and fine-grained Class C steel plates was studied over a wide range of rolling temperatures and reductions. Charpy V-notch 15 foot-pound (T_{V-15}) and 50 percent fibrous ($T_{V-50\%}$) transition temperatures were found to be much more sensitive to rolling history than the tensile ductility-transition temperatures.

Lower rolling temperatures, down to about 1450°F, improved the notch toughness equally for both steels. Refinement of the ferrite grain size over a limited range was primarily responsible for this improvement, the grain size dependence of T_{V-15} being -20°F (11°C)/ASTM No. The transition temperatures of Class C plates were uniformly lower than those of Class B for reason of differences in chemical composition.

The extra-grain-size effect of microfissuring on transition temperature, reported earlier, was too subtle for clear observation here, though good correlations were established between tensile fracturing anisotropy and mechanical fibering intensity. The fine-scale inclusion fiber structure important in this connection was identified by high-magnification electron microscopy.

Residual cold work in varying amounts in plates rolled below 1450°F had an embrittling effect; a similar but much smaller effect has been associated with the crystallographic texture in these plates.

Heavy reduction at about 1450°F is indicated as having the most potential for improvement of notch toughness. This would involve a substantial lowering of finishing temperature and would probably represent even more radical departure from the conventional than found in current "controlled rolling" practice.

Normalizing destroyed the grain refinement achieved in Class B plates by low-temperature finishing, but no effect on Class C plates studied. Effects of annealing and homogenizing treatments on T_{V-15} were consistent with a change in ferrite grain size.

There were no significant correlations between the volume-fraction, patch size, or interlammellar spacing of pearlite, on the one hand, and rolling history, heat treatment, or transition temperature, on the other. Embrittlement was observed after subcritical annealing, which is believed to bear some relationship to the resulting spheroidization of cementite.

ACKNOWLEDGMENTS

This work was part of a continuing program of research sponsored by the Ship Structure Committee and under the advisory guidance of a Project Advisory Committee of the Ship Hull Research Committee of the National Academy of Sciences-National Research Council.

REFERENCES

1. J. M. Hodge, R. D. Manning and H. M. Reichhold, "The Effect of Ferrite Grain Size on Notch Toughness", Journal of Metals, Vol. 1, 1949, p. 233.

2. R. W. Vanderbeck, "Evaluating Carbon Steels by the Keyhold Charpy Impact Test", Welding Journal, Vol. 30, 1951, p. 59-s.

3. R. H. Frazier, F. W. Boulger and C. H. Lorig, "Influence of Heat Treatment on the Ductile-Brittle Transition Temperature of Semikilled Steel Plate", Transactions AIME, Vol. 203, 1955, p. 323.

4. M. W. Lightner and R. W. Vanderbeck, "Factors Involved in Brittle Fracture", AISI Regional Technical Meetings, 1956, p. 427.

5. W. S. Owen, D. H. Whitmore, M. Cohen and B. L. Averbach, "Relation of Charpy Impact Properties to Microstructure of Three Ship Steels", Welding Journal, Vol. 36, 1957, p. 503-s.

6. F. De Kazinczy and W. A. Backofen, "Influence of Hot-Rolling Conditions on Brittle Fracture in Steel Plate", Transactions ASM, Vol. 53, 1961, p. 55.

7. J. H. van der Veen, "Influence of Steel-Making Variables on Notch Toughness", Ship Structure Committee, SSC-128, 1960.

8. B. M. Kapadia, A. T. English and W. A. Backofen, "Influence of Mechanical Fibering on Brittle Fracture in Hot-Rolled Steel Plate", Transactions ASM, Vol. 55, 1962, p. 389.

9. F. W. Boulger and W. R. Hansen, "The Effect of Metallurgical Variables in Ship-Plate Steels on the Transition Temperatures in the Drop-Weight and Charpy V-Notch Tests", Ship Structure Committee, SSC-145, 1962.

10. J. H. van der Veen, "Conference on Brittle Fracture in Steel", Journal of the West of Scotland Iron and Steel Institute, Vol. 60, 1952-53, p. 350.

11. R. W. Vanderbeck, "Controlled Low-Temperature Hot-Rolling as Practised in Europe", Welding Journal, Vol. 37, 1958, p. 114-s.

12. A. B. Kinzel and W. Crafts, "Inclusions and Their Effect on Impact Strength of Steel", Transactions AIME, Vol. 95, 1931, p. 143.

13. C. Wells and R. F. Mehl, "Transverse Mechanical Properties in Heat-Treated Wrought Steel Products", Transactions ASM, Vol. 41, 1949, p. 715.

14. W. A. Backofen and B. B. Hundy, "Mechanical Anisotropy in Some Ductile Metals", Journal of the Institute of Metals, Vol. 81, 1952-53, p. 433.

15. W. A. Backofen, "Mechanical Anisotropy in Copper", Transactions ASM, Vol. 46, 1954, p. 655.

16. E. P. Klier, F. C. Wagner and M. Gensamer, "The Correlation of Laboratory Tests with Full Scale Ship Plate Fracture Tests", Welding Journal, Vol. 27, 1948, p. 71-s.

17. W. T. Lankford, "Effect of Cold Work on the Mechanical Properties of Pressure Vessel Steels", Welding Journal, Vol. 35, 1956, p. 195-s.

18. American Bureau of Shipping Specifications for Structural Steel for Hulls, 1955.

19. J. H. van der Veen, Royal Netherlands Blast Furnaces and Steelworks, Holland. Private Communication.

20. C. S. Smith and L. Guttman, "Measurement of Internal Boundaries in Three-Dimensional Structures by Random Sectioning", Transactions AIME, Vol. 197, 1953, p. 81.

21. J. J. B. Rutherford, R. H. Aborn and E. C. Bain, "Grain Areas on a Plane Section and the Grain Size of a Metal", Metals and Alloys, Vol. 8, 1937, p. 345.

22. R. A. Grange, "Microstructural Alterations in Iron and Steel During Hot Working", paper presented to Ninth Sagamore Ordnance Materials Research Conference, New York, 1962; to be published in Conference Proceedings.

23. A. T. English and W. A. Backofen, "Recrystallization in Hot-Worked Silicon-Iron", Trans. Met. Soc. AIME, Vol. 230, p. 396, 1964.

24. C. Rossard and P. Blain, "Une Methode de Simulation par Torsion Permettant de Determiner l'Influence sure la Structure de l'Acier de ses Conditions de Laminage a Chaud", Rev. Met., Vol. 59, 1962, p. 223.

25. C. Rossard and P. Blain, "A Method of Simulation by Torsion for Determination of the Influence of Hot-Rolling Conditions on the Structure of Steel", Proceedings of the Fourth AIME Mechanical Working Conference on Flat Rolled Products, Chicago, 1962, p. 3.

26. M. A. Grossman, "Grain-Size in Metals, with Special Reference to Grain Growth in Austenite", Grain Size Symposium, ASM, Cleveland, 1934, p. 861.

27. F. B. Pickering, "Some Effects of Mechanical Working on the Deformation of Non-Metallic Inclusions", Journal of Iron and Steel Institute, Vol. 189, 1958, p. 148.

28. M. Baeyertz, "Nonmetallic Inclusions in Steel", ASM, Cleveland, 1947, p. 94.

29. L. G. Schulz, "A Direct Method of Determining Preferred Orientation of a Flat Reflection Sample Using a Geiger Counter X-Ray Sprectrometer", Journal of Applied Physics, Vol. 20, 1949, p. 1030.

30. M. Gensamer and R. F. Mehl, Transactions AIME, Vol. 120, 1936, p. 277.

31. M. Gensamer and P. A. Vukmanic, "Preferred Orientations in Hot-Rolled Low Carbon Steel", Transactions AIME, Vol. 125, 1937, p. 507.

32. W. F. Hosford and W. A. Backofen, "Strength and Plasticity of Textured Metals", in Proceedings of the Ninth Army Materials Research Conference, Syracuse University Press, 1964.

33. N. J. Petch, "The Cleavage Strength of Polycrystals", Journal of Iron and Steel Institute, Vol. 174, 1953, p. 25.

34. R. D. Stout and L. J. McGeady, "Notch Severity of Welded Steel Plate", Welding Journal, Vol. 28, 1949, p. 1-s.

35. N. F. Mott, "Mechanical Strength and Creep in Metals", Imperfections in Nearly Perfect Crystals, Wiley, New York, 1952, p. 173.

36. J. A. Rinebolt, "The Effect of Pearlite Spacing on Transition Temperature of Steel at Four Carbon Levels", Transactions ASM, Vol. 46, 1954, p. 1527.

37. J. A. Rinebolt, "Effect of Metallurgical Structures on the Impact Properties of Steels", Symposium on Effect of Temperature on the Brittle Behaviour of Metals with Particular Reference to Low Temperatures, ASTM Special Technical Publication No. 158, 1954, p. 203.

38. J. A. Rinebolt and W. J. Harris, "Effect of Alloying Elements on Notch Toughness of Pearlitic Steels", Transactions ASM, Vol. 43, 1951, p. 1175.

39. C. J. McMahon, "Micromechanisms of Cleavage Fracture in Polycrystalline Iron", Sc. D. Thesis, Department of Metallurgy, M.I.T., 1963.

40. P. J. Forsyth and D. A. Ryder, "Some Results Obtained from the Electron Microscopic Examination of the Fracture Surface of Alloys", European Regional Conference on Electron Microscopy, Delft, 1960, p. 473.

41. C. Crussard, J. Plateau and G. Henry, "Study of Mechanisms of Intergranular Fracture", Conference on Properties of Grain Boundaries, Saclay, France, 1960, p. 33.

42. A. Hayes and J. Chipman, "Mechanism of Solidification and Segregation in Low-Carbon Rimming-Steel Ingot", Transactions AIME, Vol. 135, 1939, p. 85.

43. M. Baeyertz, "Effects of Initial Structure on Austenite Grain Formation and Coarsening", Trans. ASM, Vol. 30, 1942.

44. J. W. Halley, "Grain-Growth Inhibitors in Steel", Transactions AIME, Vol. 167, 1946, p. 224.

45. M. A. Grossman, "On Grain-Size and Grain-Growth", Transactions ASST, Vol. 21, 1933, p. 1079.

46. E. S. Davenport and E. C. Bain, "General Relation Between Grain-Size and Hardenability and the Normality of Steels", Grain Size Symposium, ASM, Cleveland, 1934, p. 879.

47. D. A. Canonico, E. H. Kottcamp, and R. D. Stout, "Accelerated Cooling of Carbon Steels for Pressure Vessels", Welding Journal, Vol. 40, 1961, p. 400-s.

48. United States Steel Corporation, "Fine-Grained, Heat-Treated, Wrought Medium-Carbon Steel", U. S. Patent, 1959.

APPENDIX

Further Detail on Materials and Procedure, Microstructure Data and Test Results

TABLE IA. PLATE IDENTIFICATION AND PROCESSING DATA.

ABS Class B, 1-1/2-inch thickness+

Rolling Practice	Plate Identification Number	Reduction in Thickness, %	Average Measured Finishing Temperature,* °F	Temperature Change during Rolling, °F
Isothermal	2	15.2	1950	-100
"	19	15.0	1640	- 60
"	10	15.0	1445	- 45
"	25	14.9	1275	- 15
Isothermal	8	30.1	1945	- 90
"	16	29.8	1640	- 40
"	13	29.7	1445	- 35
"	9	29.8	1260	- 20
Isothermal	6	59.3	1950	- 55
"	11	59.0	1650	- 40
"	20	59.0	1450	+ 15
"	23	58.6	1260	+ 40
Non-isothermal	12	29.8	1595**	-230
"	22	29.7	1455**	-195
"	1	29.8	1250**	-205

ABS Class C, 1-1/4-inch thickness+

Isothermal	7	21.0	1980	----
"	8	20.8	1800	----
"	9	20.9	1600	----
Isothermal	2	51.2	2035	- 30
"	3	50.1	1815	+ 10
"	4	49.8	1595	- 10
Conventional	12	52.0	1800**	- 290

+ Class B plates were air-cooled to isothermal finishing temperatures after preliminary rolling above 2000°F. Class C plates, on the other hand, were cooled to room temperature, reheated to 2050°F and held for two hours before isothermal finishing.

* Temperatures were measured continuously during rolling by shielded, chromel-alumel thermocouples inserted in 3-inch-deep holes drilled at midthickness in one side of each plate.

** Temperature of the finishing pass. Plate C-12 was given the last 50% of its reduction with temperature gradually dropping from 2090°F to 1800°F.

CHARPY TESTS - EXPERIMENTAL DETAILS AND STATISTICAL ANALYSIS

Charpy specimens were tested at temperatures from 212°F to -60°F. For cooling below room temperature a mixture of acetone and dry ice was used, while a water bath was used for higher temperatures. The specimens were held at temperatures for about 15 minutes and broken within 4 seconds after removal from the bath. A 264 foot-pound Tinius Olsen testing machine with striking velocity of approximately 17 feet per second was employed. The fracture surfaces of the broken bars were examined under a stereoscopic microscope at low magnification (7X), and the amount, in percent, of fibrous portion of the fracture was estimated. From the energy absorbed and percent fibrous vs. temperature plots, the T_{V-15} and $T_{V-50\%}$ were determined. Typical curves are shown in Figure 1A for plates B-9 and B-20. Altogether two bars were machined from the plate thickness, and were evenly spaced to minimize the effect of variation in microstructure. No correlation was found between the scatter and location of specimens in the plate.

The experimental uncertainties in transition temperatures have been estimated on a statistical basis using the values of standard deviations established earlier by Rinebolt and Harris,[1]* with the assumption that the same magnitude of scatter is involved. From results of extensive testing they calculated the standard deviation (σ) of the T_{V-15} and $T_{V-50\%}$, with five specimens tested in the transition region, to be 8.2°F and 14.0°F, respectively. With twelve specimens being used instead in these experiments, the standard deviations were adjusted** to 5.3°F and 9.0°F, respectively. The uncertainty in transition temperatures is then given by $\pm 2\sigma$ with 95 percent confidence, or $\pm$ 10.6°F (6°C) and $\pm$ 18°F (10°C), respectively, in the two cases. Further, the difference between two transition temperatures must exceed 2.38σ if it is to be significant with 95 percent confidence, or 15°F (8.3°C) and 25°F (14°C), respectively.

REPLICATION TECHNIQUE FOR ELECTRON MICROFRACTOGRAPHY

Chromium-shadowed, negative carbon replicas of the fracture surfaces were prepared by a two-stage technique, which was essentially a modification of one described by Bradley.[2,3] First, a 0.0075 in. thick cellulose acetate strip, softened with a drop of acetone, was moulded under pressure against the fracture surface, and allowed to dry. This was then carefully stripped, and the step repeated once more to clean the surface before obtaining a usable replica. Next, a thin layer of chromium (approximately 50 A° thick) was deposited on the replica by vacuum evaporation at approximately 25° to the replica plane. This was followed by a thin deposit of carbon by "rotary shadowing" at nearly normal incidence. Finally, the replica was placed with its cellulose acetate side down on an electron microscope specimen - grid supported by a fine mesh screen. The latter was then

---

* References appear at end of Appendix.

** Standard deviation of a mean of n values = $\frac{\sigma}{\sqrt{n}}$

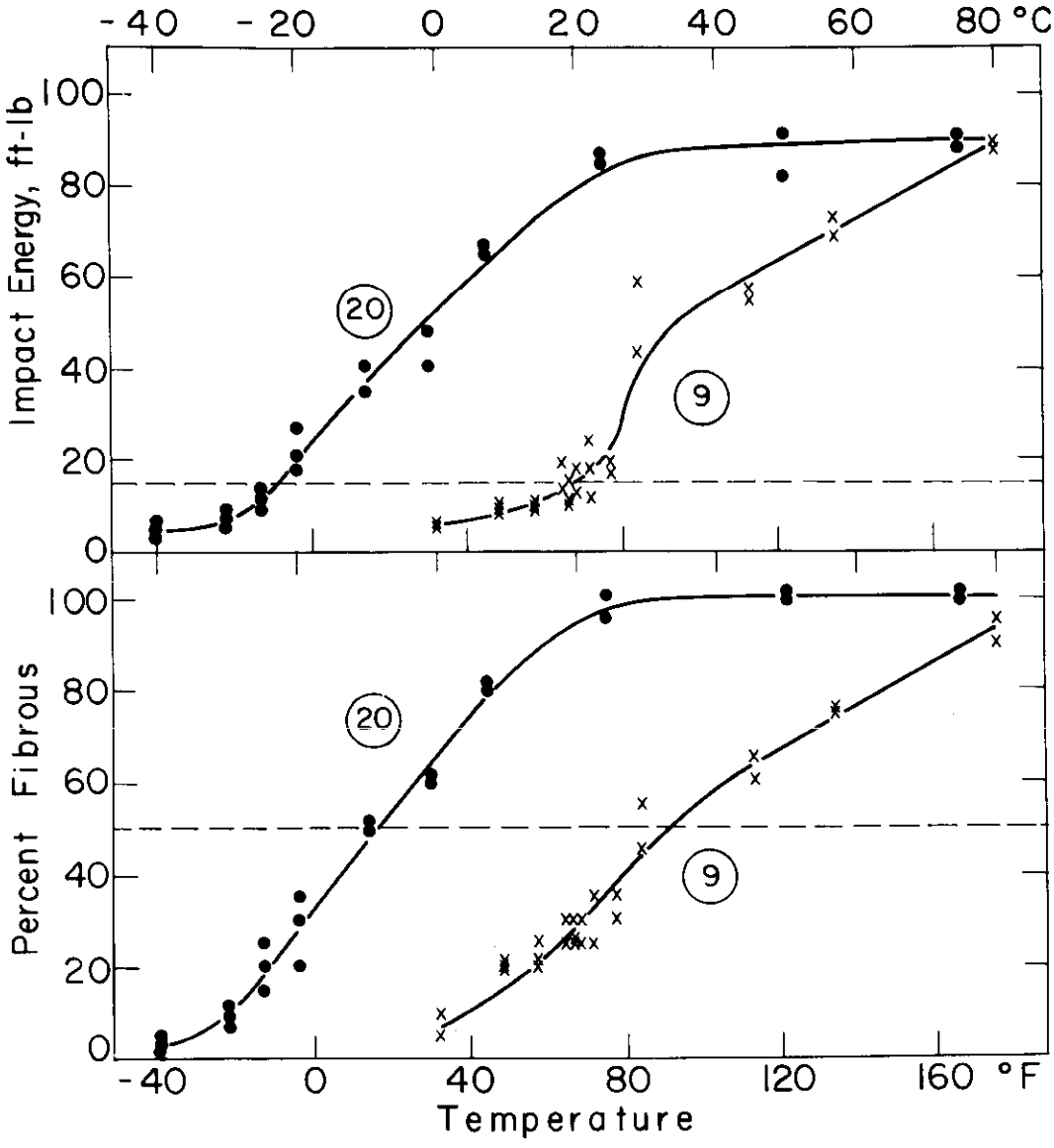

Fig. 1A. Representative Charpy V-notch Test Data From Class B Plates 9 and 20, Showing Determination of T_{v-15} *and* $T_{v-50\%}$

placed on the surface of an acetone bath (so that the replica is wetted by, but not submerged in, the acetone) to dissolve away the acetate, leaving behind a chromium - shadowed, negative carbon replica to be examined.

A Siemens 100 KV electron microscope was used for the purpose. The resolving power obtained with the replication process described was about 0.05μ. Fracture surfaces at magnifications ranging from 4,000X to 40,000X could be successfully examined.

TABLE IIA. MICROSTRUCTURAL AND HARDNESS DATA.

ABS Class B, Heat-treated

Plate Number+	Heat-treatment	Grain Size, ASTM Number		Inclusion Count, q	Pearlite Volume %	Pearlite Patch Size, mm	Widmanstätten Structure, Volume %	Hardness, Rockwell B
		R-T-Z	T-Z					
2a	Normalizing	7.40	7.45	43	24.0	0.016	35	69.0
10a	"	7.45	7.45	57	25.5	0.018	15	68.0
25a	"	6.95	7.15	62	24.5	0.0185	10	68.0
16a	"	7.00	7.00	44	26.0	0.017	25	68.0
9a	"	7.55	7.50	55	24.0	0.015	10	67.0
20a	"	7.50	7.50	88	27.0	0.0175	10	67.5
10B	Full-Annealing	5.60	5.80	45	28.0	0.035	0	62.0
20C	" "	5.75	6.00	69	25.0	0.033	0	61.0
8e	Subcritical Annealing	6.70	6.70	44	23.5*	0.017*	0	60.0
9f	" "	6.90	7.10	70	25.0*	0.018*	0	63.0
9F	" "	6.50	6.75	41	23.0*	0.018*	0	66.5
16F	" "	7.60	7.65	60	21.0*	0.0145*	0	62.0
8g	" "	6.35	6.35	47	23.0*	0.0175*	0	57.5
8G	" "	6.20	6.20	49	18.5*	0.0185*	0	57.5
8H	Homogenizing	4.20	4.20	20	23.5	0.050	5	62.0
8Haa	H-N-N	7.25	7.25	18	27.0	0.018	20	68.0
8HaA	H-N-A	5.80	5.80	22	26.0	0.038	0	59.0

ABS Class C, Heat-treated

4a	Normalizing	8.65	8.65	55	18.0	0.011	0	69.0
7a	"	8.50	8.50	42	21.0	0.0115	0	66.5
4f	Subcritical Annealing	8.20	8.20	77	19.0*	0.0135*	0	64.5
7f	" "	6.90	6.90	66	21.0*	0.0165*	0	62.5

+ Numbers indicate rolling histories and heat-treatments listed in Tables II and III, respectively.

* Refers to partially or completely spheroidized areas.

EXPLANATION OF FOOTNOTES

+ Numbers indicate rolling histories listed in Table II.
ϕ There was a noticeable gradation in microsturcture across plate thickness. In general, smaller grain-size and larger amounts of pearlite and Widmanstätten areas were observed near the surface than at the center; above values represent average measurements.
++ Average of at least five measurements.
* Rockwell-B hardness measurements were made along the width and thickness of the plates. Hardness at the center was smaller than that at the surface, up to a maximum of 6.0 units; the average values are given above.
** Values subject to large scatter due to strong banding.

STABILITY OF AUSTENITE DURING ROLLING AT 1450°F

Depending on the rate of cooling, the upper critical temperature in steel (Ar_3) is depressed more or less below its equilibrium value (Ae_3). For example, in a steel of similar composition to that used here, the Ar_3 for cooling at the rate of 25°F per minute was lowered to approximately 1390°F compared to the Ae_3 value of about 1550°F.[4] The over-all rate of

TABLE IIA (CONTINUED) MICROSTRUCTURAL AND HARDNESS DATA.

ABS Class B

Plate Number+	Grain Size,♦ ASTM Number		Inclusion++ Count, q	Pearlite,♦ Volume %	Pearlite Patch Size, mm	Widmanstätten♦ Structure, Volume %	Hardness,* Rockwell-B
	R-T-Z	T-Z					
2	6.45	6.60	43	22.0	0.0215	5	64.0
19	6.95	7.10	55	21.0	0.020	5	63.0
10	7.80	7.80	57	26.5	0.015	5	69.5
25	6.80	6.90	49	23.5	0.016	15	74.0
8	6.50	6.70	38	22.5	0.021	0	63.0
16	7.40	7.55	62	23.5	0.018	0	69.0
13	7.90	7.90	57	25.5	0.015**	0	68.0
9	7.30	7.55	66	23.0	0.015	15	74.0
6	7.15	7.15	51	22.5	0.0185	0	66.0
11	7.40	7.40	66	20.0	0.018**	0	69.5
20	8.65	8.65	103	23.0	0.015**	0	69.5
23	6.60	7.45	106	24.0	0.019	15	79.0
12	7.10	7.25	48	20.5	0.0155	0	64.5
22	7.60	7.70	67	20.5	0.014	0	67.0
1	7.80	8.00	70	23.5	0.014	5	75.0

ABS Class C

7	7.15	7.15	56	22.0	0.016	5	66.0
8	7.00	7.05	73	21.5	0.0165	5	66.0
9	7.55	7.60	61	23.0	0.015	0	67.0
2	7.40	7.45	92	21.0	0.015	0	67.0
3	7.75	7.75	93	21.5	0.015	0	66.5
4	8.30	8.40	90	22.5	0.015	0	66.5
12	7.70	7.80	87	21.0	0.015	0	70.0

cooling from Ae_3 down to 1390°F for the plates rolled at 1450°F in this work may be approximately equated to

$$\left[\frac{1550 - 1390}{\left(\frac{1550 - 1390}{50}\right) + 1.5} \right] \simeq 34^{\circ}F \text{ per minute}$$

where the $\left(\frac{1550 - 1390}{50}\right)$ in the denominator is the time for air cooling at a

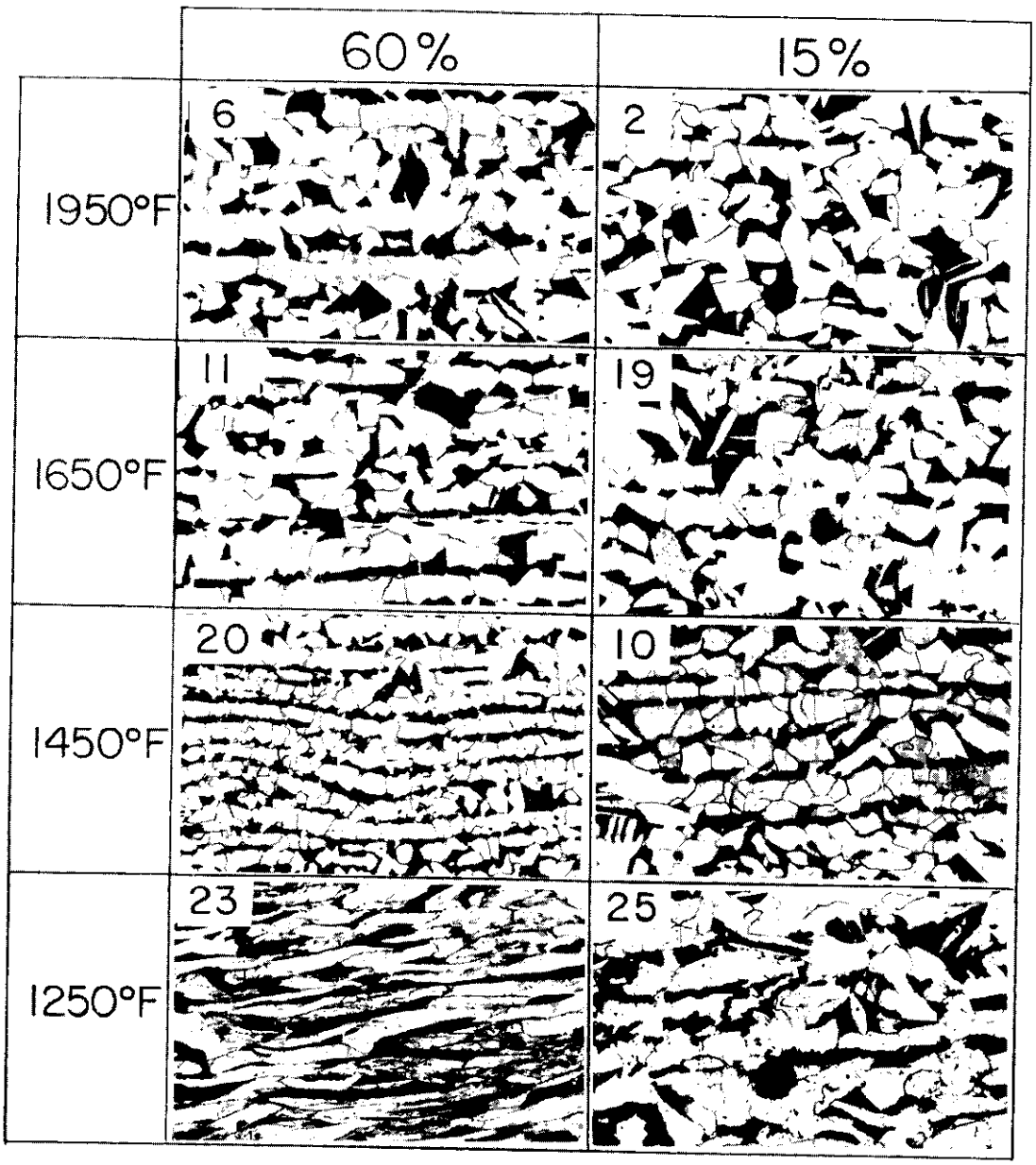

Fig. 2A. Microstructures of As-Rolled Class B Plates (R-Z Plane). 2% Nital etch. 135X

rate of about 50°F per minute,[5] and 1.5 is the time in minutes for the six passes in the reduction schedule.[5]

The Ar_3 at this cooling rate should be even lower than 1390°F. Since at the termination of rolling, the plate temperature ranged from approximately 1450°F at center to 1400°F at the surface, the austenite transformation probably did not begin until some time after completion of rolling.

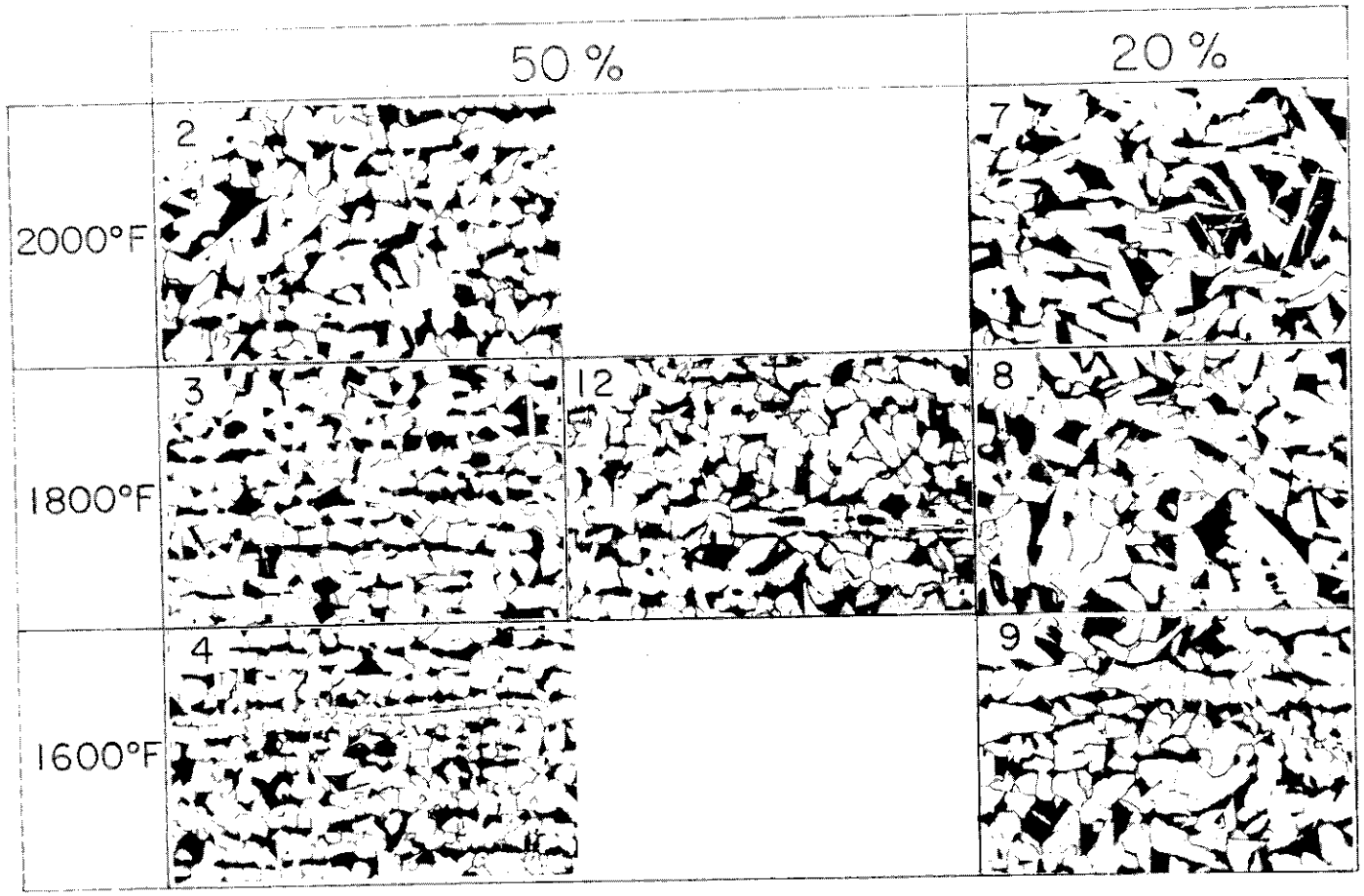

Fig. 2A (continued). Microstructures of As-Rolled Class C Plates (R-Z Plane). 2% Nital etch 135 X

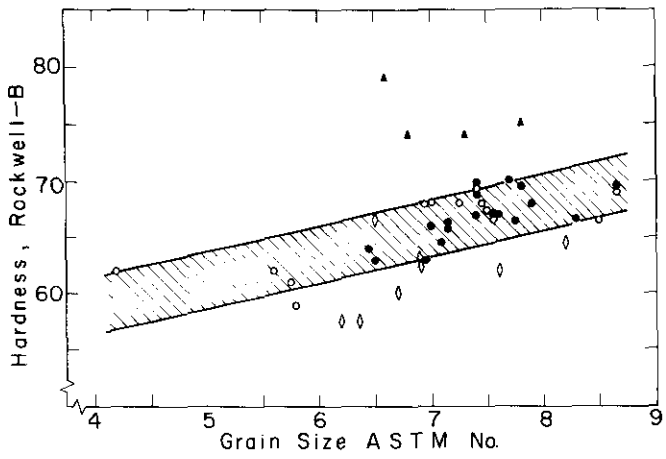

Fig. 3A. Grain Size Dependence of Rockwell-B Hardness for Class B and Class C Plates in As-Rolled (●) and Heat-treated (○) Condition. Plates rolled at 1250 F (▲) were significantly harder than others owing to residual cold work, while those subcritically annealed at 1250 F (◇) had somewhat lower hardness because of spheroidization of cementite.

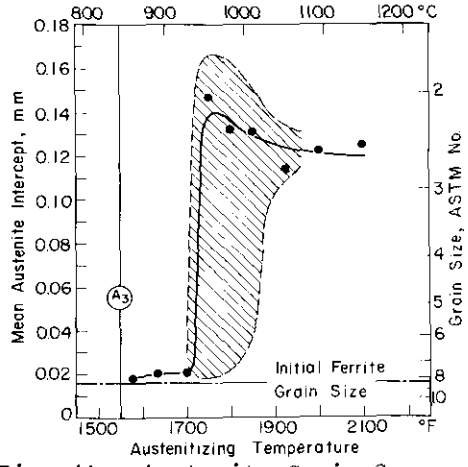

Fig. 4A. Austenite Grain Coarsening Behavior in Class C Steel. Shaded area approximately represents duplex grain-size field. A_3 locates the equilibrium value of the upper critical temperature.

AUSTENITE GRAIN COARSENING IN CLASS C STEEL

The austenite grain-coarsening behavior of ABS class C fine-grained steel was studied by austenitizing samples for 1 hour at temperatures from 1580°F to 2100°F, and rapidly quenching in water. On etching with a 5 percent aqueous solution of ferric chloride, the resulting microstructure was observed to consist of low-carbon martensite with a network of ferrite at the prior austenitic grain boundaries. The coarsening temperature was observed to be about 1725°F, at which the average austenite grain size underwent a sharp increase from 8.0 ASTM No. to nearly 2.0 ASTM No., as shown in Figure 4A.

THEORETICAL IMPLICATIONS

The $T_{V\text{-}15}$ measurements relating to the grain-size effect and two of the extra-grain-size effects can be rationalized to some degree with current fracture theory. The occurrence of brittle fracture is influenced by factors which govern plastic yielding; according to Cottrell,[6] the condition for ductile-brittle transition is defined by the equation:

$$\sigma_y \, k_y \, d^{1/2} = \beta \, \gamma \, \mu \qquad \text{(I)}$$

TABLE IIIA. TENSILE RESULTS.

ABS Class B

Plate Number+	* Ductility-Transition, °F		Fracturing Anisotropy Ratios++			
	Thickness (Z) Direction	Rolling (R) Direction	$(\frac{\epsilon_Z}{\epsilon_R})_{RT}$	$(\frac{\sigma_Z}{\sigma_R})_{RT}$	$(\frac{\sigma_Z}{\sigma_R})_{max}$	$(\frac{\sigma_Z}{\sigma_R})^*$
2	-315	-324	0.50	0.63	0.78	0.97
19	-297	-333	0.37	0.60	0.62	0.87
10	-315	-315	0.39	0.62	0.69	1.00
25	-297	-315	0.45	0.62	0.74	0.88
8	-315	-324	0.51	0.62	0.71	0.92
16	-297	-351	0.30	0.55	0.58	0.78
13	-297	-333	0.47	0.61	0.66	0.81
9	-243	-315	0.39	0.60	0.63	0.76
6	-306	-333	0.48	0.65	0.66	0.88
11	-297	-351	0.30	0.57	0.60	0.78
20	-261	-342	0.25	0.52	0.57	0.68
23	-180	-333	0.31	0.59	0.53	0.57
12	-333	-333	0.45	0.62	0.68	1.00
22	-270	-342	0.41	0.59	0.66	0.77
1	-288	-333	0.39	0.60	0.65	0.83

+ Numbers indicate rolling histories listed in Table II.

++ RT represents room temperature.
The "max" subscript means that values were obtained from the peaks of the stress vs. temperature curves.
The * symbol means that the ratio is formed of stress values at the ductility-transition temperatures.

TABLE IIIA (CONTINUED). TENSILE RESULTS.

ABS Class C

Plate Number+	Fracturing Anisotropy Ratios++	
	$(\frac{\epsilon_Z}{\epsilon_R})_{RT}$	$(\frac{\sigma_Z}{\sigma_R})_{RT}$
7	0.210	0.58
8	0.121	0.47
9	0.157	0.52
2	0.113	0.45
3	0.121	0.44
4	0.110	0.44
12	0.146	0.52

+ Numbers indicate rolling hisotries listed in Table II.

++ RT represents room temperature.

where σ_y is the lower yield stress, k_y is a dislocation locking strength parameter, d is mean grain diameter, β is a constant depending on the type of stress system, γ is the effective surface energy, and μ is the shear modulus. When the left-hand side exceeds the right-hand side, depending on temperature and strain-rate, the condition for crack growth is satisfied and brittle fracture results. The critical temperature at which the condition is just satisfied for a given strain-rate is the ductility transition temperature; such a temperature can probably be identified with the 15 foot-pound level in a Charpy V-notch test (T_{V-15}). For a given material, equation I predicts the transition temperature to be a function of grain-size, the friction stress on a free dislocation, σ_i, the dislocation locking strength, and the degree of triaxiality of stress. Predictions of the theory have been found to be in reasonable quantitative agreement with experimental measurements with studies of transition temperature in relation to grain-size, strain-rate, and radiation.[6,7] Petch[8] has derived a similar equation for the fracture mode transition from ductile to cleavage; this also gave reasonable explanations of the effect on transition temperature of grain-size, quench-aging, prestrain, and strain-aging.

In the present work, ferrite-grain-size appears as the major structural variable affecting transition temperature. Using theory at hand, the grain-size dependence of T_{V-15} found here can be rationalized.

Differentiating equation I, assuming that $\beta\,\gamma\,\mu$ is in fact a constant,

$$\frac{\Delta T_{V-15}}{\Delta d^{-1/2}} = - \frac{\partial (\sigma_y\, k_y\, d^{1/2}) / \partial d^{-1/2}}{\partial (\sigma_y\, k_y\, d^{1/2}) / \partial T}$$

$$= - \frac{k_y\, d^{1/2}\, (\frac{\partial \sigma_y}{d^{-1/2}}) + \sigma_y\, k_y\, (\frac{\partial d^{1/2}}{\partial d^{-1/2}})}{k_y\, d^{1/2}\, (\frac{\partial \sigma_y}{\partial T}) + \sigma_y\, d^{1/2}\, (\frac{\partial k_y}{\partial T})}$$

According to the limited data in Table IV, k_y is independent of temperature. Therefore,

$$\frac{\Delta T_{V-15}}{\Delta d^{-1/2}} = - \left[\frac{k_y^2 \cdot d^{1/2} - \sigma_y\, k_y\, d}{k_y\, d^{1/2}\, (\frac{\partial \sigma_y}{\partial T})} \right]$$

$$= \frac{\sigma_i\, d^{1/2}}{(\frac{\partial \sigma_y}{\partial T})} \qquad \text{(II)}$$

TABLE IVA. CHARPY RESULTS.

ABS Class B

Plate Number+	T_{V-15} (°F)	$T_{V-50\%}$ (°F)
2	30	72
19	25 (34*)	55 (55*)
10	9	52
25	54 (73*)	93 (99*)
8	30	82
16	10	39
13	16	41
9	68	91
6	18	59
11	12	50
20	- 9	16
23	57	73
12	23	68
22	1	41
1	37	64

ABS Class C

7	0	61
8	- 4	57
9	- 9	52
2	-17	41
3	-20	34
4	-29	18
12	- 8	61

ABS Class B, Heat Treated

Plate Number+	T_{V-15} (°F)	$T_{V-50\%}$ (°F)
2a	36	82
10a	25	72
25a	32	75
16a	30	82
9a	28	68
20a	14	68
10B	46	86
20C	45	82
8e	48	91
9f	57	108
9F	61	91
16F	37	68
8g	82	140
8G	82	133
8H	75 (75*)	131 (127*)
8Haa	36	99
8HaA	50 (50*)	100 (100*)

ABS Class C, Heat Treated

4a	-31	9
7a	-29	18
4f	- 6	43
7f	27	79

+ Numbers indicate rolling histories listed in Table II.

* Specimens taken along transverse direction in the plate with notch along the thickness direction.

Evaluating the right-hand side requires data for both numerator and denominator taken under conditions existing near the notch root in a Charpy bar at the ductility transition temperature (T_{V-15}). The best supply of such data would come from smooth-bar tension tests as a function of temperature at the characteristic Charpy strain-rate. Unfortunately, those experiments have not been made. According to one interpretation of the theory, however, the important thing to know is the value of σ_y at transition--in the presence of a notch in the Charpy example. The reason is that if k_y is neither temperature nor strain-rate dependent, and grain-size is fixed by considering a given material, only σ_y is left to satisfy the left-hand side of equation I. Now, ductility transition temperatures have been measured using low strain-rate notched-tension tests; in light of the preceding remark, σ_y under these conditions ought to be the same as that prevailing at the Charpy notch-root. Of course, the temperature for notched-tension transition will be lower owing to the lower strain-rate, but σ_y should be the same. Going further, the notched-tension ductility transition usually falls about 180°F higher than the smooth-bar tensile-ductility transition;[6] in the present work, the latter temperature is -230°F on the average (Figure 8, R data). Therefore the notched-tension temperature

would have been about -150°F, had it been measured. The conventional tensile-yield vs. $d^{-1/2}$ plots contain one for -145°F; the σ_i value at this temperature (Table IV) is close to 36,100 psi; that value would be introduced in equation II. From all σ vs. T plots (examples shown in Figure 5), the average $(\partial \sigma_y / \partial T)$ at -150°F was approximately -250 psi per °F. Finally, choosing $d^{1/2} = 0.19$ millimeter$^{1/2}$ for an ASTM grain-size number 7.5, the grain-size dependence of T_{V-15} that comes from equation II is equal to -27.5°F per millimeter$^{-1/2}$, or - 26°F per ASTM number, which is in reasonable agreement with the experimental dependence of -20°F per ASTM number.

The amount of cold-work embrittlement, rated as an increase in T_{V-15} for fixed grain-size, was estimated for each of the 1250°F finished plates. Average values of the friction stress increment, $\overline{\Delta \sigma_i}$, for each plate given in Table IV are repeated in Table VA; the corresponding rise in T_{V-15} observed experimentally (extra-grain-size embrittlement) is included for comparison. Differentiating equation I,

$$\frac{\Delta T_{V-15}}{\Delta \sigma_i} = - \frac{\partial(\sigma_y k_y d^{1/2})/\partial \sigma_i}{\partial(\sigma_y k_y d^{1/2})/\partial T}$$

$$= - \left[\frac{k_y d^{1/2} \left(\frac{\partial \sigma_y}{\partial \sigma_i}\right)}{k_y d^{1/2} \left(\frac{\partial \sigma_y}{\partial T}\right) + \sigma_y d^{1/2} \left(\frac{\partial k_y}{\partial T}\right)} \right]$$

$$= - \frac{1}{\left(\frac{\partial \sigma_y}{\partial T}\right)}$$

TABLE VA. COLD WORK EMBRITTLEMENT.

Plate Number+	Rolling History	Average Increment in Friction Stress, $\overline{\Delta \sigma_i}$ (1000 psi)	ΔT_{V-15} (°F)	
			Experimental	Calculated
B-23	60% at 1250°F, ISO.	16.0	43	64
B-9	30% at 1250°F, ISO.	12.0	56	48
B-25	15% at 1250°F, ISO.	5.5	27	22
B-1	30% at 1250°F, NON-ISO.	6.5	34	26

+ Number indicate rolling histories listed in Table II.

on simplifying, since k_y is again independent of temperature. Substituting for $(\partial \sigma_y / \partial T)$ as before:

$$\Delta T_{V-15} \ (^{o}F) = 0.004 \Delta \sigma_i \qquad \text{(III)}$$

Values of ΔT_{V-15} (^{o}F) were calculated from equation III for each plot, and results compared with experimental values in Table VA, are in reasonable agreement.

REFERENCES

1. J. A. Rinebolt and W. J. Harris, "Statistical Analysis of Tests of Charpy V-Notch and Keyhole Bars", Welding Journal, Vol. 30, 1951, p. 202.

2. D. E. Bradley, "Evaporated Carbon Replica Technique for Electron Microscope", Journal of the Institute of Metals, Vol. 83, 1954-55, p. 35.

3. D. E. Bradley, "Some Advances with Evaporated Carbon Replica Technique", Proceedings of the International Conference on Electron Microscopy, London, 1954, p. 478.

4. J. A. Rinebolt and W. J. Harris, "Effect of Alloying Elements on Notch Toughness of Pearlitic Steels", Transactions American Society for Metals, Vol. 43, 1951, p. 1175.

5. R. M. Brown, Applied Research Laboratory, United States Steel Corporation, Pittsburgh; Private communication.

6. A. H. Cottrell, "Theory of Brittle Fracture in Steel and Similar Metals", Transactions AIME, Vol. 212, 1958, p. 192.

7. A. T. Churchman, I. Mogford and A. H. Cottrell, "The Hardening and Embrittlement of Steel by Irradiation with Neutrons", Philosophical Magazine, Vol. 2, 1957, p. 1271.

8. N. J. Petch, "The Ductile-Cleavage Transition in Alpha-Iron", Proceedings of the International Conference on the Atomic Mechanisms of Fracture, Wiley, New York, 1959, p. 54.

NONE

Security Classification

DOCUMENT CONTROL DATA - R&D

(Security classification of title, body of abstract and indexing annotation must be entered when the overall report is classified)

1. ORIGINATING ACTIVITY *(Corporate author)*

Ship Structure Committee

2a. REPORT SECURITY CLASSIFICATION

NONE

2b. GROUP

3. REPORT TITLE

ROLLING HISTORY IN RELATION TO THE TOUGHNESS OF SHIP PLATE

4. DESCRIPTIVE NOTES *(Type of report and inclusive dates)*

Final Report

5. AUTHOR(S) *(Last name, first name, initial)*

B. M. Kapadia and W. A. Backofen

6. REPORT DATE	7a. TOTAL NO. OF PAGES	7b. NO. OF REFS
May 1965	46	56

8a. CONTRACT OR GRANT NO.	9a. ORIGINATOR'S REPORT NUMBER(S)
NObs-88282	
b. PROJECT NO.	
c.	9b. OTHER REPORT NO(S) *(Any other numbers that may be assigned this report)*
d.	

10. AVAILABILITY/LIMITATION NOTICES

All distribution of this report is controlled. Qualified DDC users shall request through Ship Structure Committee, U. S. Coast Guard Headquarters, Washington, D. C.

11. SUPPLEMENTARY NOTES	12. SPONSORING MILITARY ACTIVITY
	Bureau of Ships, Dept. of the Navy Washington, D. C.

13. ABSTRACT Plates of ABS Class-B and Class-C steel were rolled with different temperature-reduction schedules to observe effects of processing history on final structure and properties. Each class was finished at a constant thickness (1-1/2-in. for Class B; 1-1/4-in. for Class C) following both isothermal and non-isothermal schedules with reductions from 15% to 60% and temperatures in the range 1250°F (677°C) to 2000°F (1093°C). The principal measurements for toughness evaluation were the 15 ft-lb V-notch Charpy, the 50%-fibrous Charpy, and the tensile-ductility transition temps.

Effects were divided into two basic categories, one concerned entirely with ferrite grain size, the other with various extra-grain-size details of structure and composition. The most significant improvements in toughness were the result of ferrite grain-size refinement. The notch toughness of both steels was increased equally for this reason as rolling temperature was lowered to 1450°F (788°C).

The superior toughness of Class C at constant grain size was an example of an extra-grain-size of composition. Normalizing of Class B plates after rolling produced Widmanstätten structure and some embrittlement which was interpreted as an apparent extra-grain-size effect of this particular heat treatment. Mechanical fibering was studied with techniques that included electron microscopy, but the contribution of microfissuring effects to toughness was too subtle for observation. Embrittlement from residual cold work as a consequence of low-temperature finishing was also identified. Results of heat treatment after rolling were studied in detail.

DD FORM 1 JAN 64 1473

NONE

Security Classification

NONE

Security Classification

14. KEY WORDS	LINK A		LINK B		LINK C	
	ROLE	WT	ROLE	WT	ROLE	WT

INSTRUCTIONS

1. ORIGINATING ACTIVITY: Enter the name and address of the contractor, subcontractor, grantee, Department of Defense activity or other organization *(corporate author)* issuing the report.

2*a*. REPORT SECURITY CLASSIFICATION: Enter the overall security classification of the report. Indicate whether "Restricted Data" is included. Marking is to be in accordance with appropriate security regulations.

2*b*. GROUP: Automatic downgrading is specified in DoD Directive 5200.10 and Armed Forces Industrial Manual. Enter the group number. Also, when applicable, show that optional markings have been used for Group 3 and Group 4 as authorized.

3. REPORT TITLE: Enter the complete report title in all capital letters. Titles in all cases should be unclassified. If a meaningful title cannot be selected without classification, show title classification in all capitals in parenthesis *immediately following* the title.

4. DESCRIPTIVE NOTES: If appropriate, enter the type of report, e.g., interim, progress, summary, annual, or final. Give the inclusive dates when a specific reporting period is covered.

5. AUTHOR(S): Enter the name(s) of author(s) as shown on or in the report. Enter last name, first name, middle initial. If military, show rank and branch of service. The name of the principal author is an absolute minimum requirement.

6. REPORT DATE: Enter the date of the report as day, month, year, or month, year. If more than one date appears on the report, use date of publication.

7*a*. TOTAL NUMBER OF PAGES: The total page count should follow normal pagination procedures, i.e., enter the number of pages containing information.

7*b*. NUMBER OF REFERENCES: Enter the total number of references cited in the report.

8*a*. CONTRACT OR GRANT NUMBER: If appropriate, enter the applicable number of the contract or grant under which the report was written.

8*b*, 8*c*, & 8*d*. PROJECT NUMBER: Enter the appropriate military department identification, such as project number, *subproject* number, system numbers, task number, etc.

9*a*. ORIGINATOR'S REPORT NUMBER(S): Enter the official report number by which the document will be identified and controlled by the originating activity. This number must be unique to this report.

9*b*. OTHER REPORT NUMBER(S): If the report has been assigned any other report numbers *(either by the originator or by the sponsor)*, also enter this number(s).

10. AVAILABILITY/LIMITATION NOTICES: Enter any limitations on further dissemination of the report, other than those *imposed by* security classification, using standard statements such as:

(1) "Qualified requesters may obtain copies of this report from DDC."

(2) "Foreign announcement and dissemination of this report by DDC is not authorized."

(3) "U. S. Government agencies may obtain copies of this report directly from DDC. Other qualified DDC users shall request through _____."

(4) "U. S. military agencies may obtain copies of this report directly from DDC. Other qualified users shall request through _____."

(5) "All distribution of this report is controlled. Qualified DDC users shall request through _____."

If the report has been furnished to the Office of Technical Services, Department of Commerce, for sale to the public, indicate this fact and enter the price, if known.

11. SUPPLEMENTARY NOTES: Use for additional explanatory notes.

12. SPONSORING MILITARY ACTIVITY: Enter the name of the departmental project office or laboratory sponsoring *(paying for)* the research and development. Include address.

13. ABSTRACT: Enter an abstract giving a brief and factual *summary of the document* indicative of the report, even though it may also appear elsewhere in the body of the technical report. If additional space is required, a continuation sheet shall be attached.

It is highly desirable that the abstract of classified reports be unclassified. Each paragraph of the abstract shall end with an *indication of the military security* classification of the information in the paragraph, represented as *(TS), (S), (C), or (U)*

There is no limitation on the length of the abstract. However, the suggested length is from 150 to 225 words.

14. KEY WORDS: Key words are technically meaningful terms *or short phrases* that characterize a report and may be used as index entries for cataloging the report. Key words must be selected so that no security classification is required. Identifiers, such as equipment model designation, trade name, military project code name, geographic location, may be used as key words but will be followed by an indication of technical context. The assignment of links, roles, and weights is optional.

NATIONAL ACADEMY OF SCIENCES-NATIONAL RESEARCH COUNCIL
DIVISION OF ENGINEERING AND INDUSTRIAL RESEARCH

The Ship Hull Research Committee undertakes research service activities in the general fields of materials, design, and fabrication, as relating to improved ship hull structure, when such activities are accepted by the Academy as part of its functions. The Committee recommends research objectives and projects; provides liaison and technical guidance to such studies; reviews project reports; and stimulates productive avenues of research.

SHIP HULL RESEARCH COMMITTEE

Chairman: RADM A. G. Mumma, USN (Ret.)
Executive Vice President
Worthington Corporation

Members:

Prof. R. B. Couch, Chairman
Dept. of Naval Architecture
& Marine Engineering
University of Michigan

Mr. Hollinshead de Luce
Asst. to Vice President
Bethlehem Steel Co.

Dr. C. O. Dohrenwend
Vice President & Provost
Rensselaer Polytechnic Inst.

Prof. J. Harvey Evans
Prof. of Naval Architecture
Mass. Institute of Technology

Professor J. E. Goldberg
Prof. of Civil Engineering
Purdue University

Mr. James Goodrich
Exec. Vice President
Bath Iron Works

Mr. D. C. MacMillan
President
George G. Sharp, Inc.

Arthur R. Lytle
Director

R. W. Rumke
Executive Secretary

SR-147 PROJECT ADVISORY COMMITTEE
"Mill Rolling Practice"

Chairman: Mr. Thomas S. Washburn
Chesterton, Indiana

Members:

Mr. J. L. Giove
Chief Metallurgist
U. S. Steel Corp.
Homestead District Works

Mr. T. T. Watson
Coatesville
Pennsylvania

Mr. J. R. LeCron
Metallurgical Engineer
Bethlehem Steel Co.

Dr. Cyril Wells
Principal Research Metallurgical
Engineer
Metal Research Laboratory
Carnegie Institute of Technology

SHIP STRUCTURE COMMITTEE PUBLICATIONS

SSC-158, Low-Stress Brittle Fracture in Mild Steel by R. Dechaene, W. Soete, and A. Vinckier. August 30, 1963. **PB 181-547 $.75

SSC-159, Acquisition and Analysis of Acceleration Data by F. C. Bailey, D. J. Fritch and N. S. Wise. February 17, 1964.

SSC-160, Geometric Effects of Plate Thickness by R. D. Stout, C. R. Roper and D. A. Magee. February 7, 1964.

SSC-161, Micromechanisms of Cleavage Fracture in Polycrystalline Iron by Charles J. McMahon, Jr. May 1964.

SSC-162, Exhaustion of Ductility and Brittle Fracture of E-Steel Caused by Prestrain and Aging by C. Mylonas. July 1964.

SSC-163, Investigation of Bending Moments within the Midships Half Lengh of a Mariner Model in Extreme Waves by N. M. Maniar. June 1964.

SSC-164, Results from Full-Scale Measurements of Midship Bending Stresses on Two C4-S-B5 Dry-Cargo Ships Operating in North Atlantic Service by D. J. Fritch, F. C. Bailey and N. S. Wise. September 1964.

SSC-165, Local Yielding and Extension of a Crack Under Plane Stress by G. T. Hahn and A. R. Rosenfield. December 1964.

SSC-166, Reversed-Bend Tests of ABS-C Steel with As-Rolled and Machined Surfaces by K. Satoh and C. Mylonas. April 1965.

SSC-167, Restoration of Ductility of Hot or Cold Strained ABS-B Steel by Treatment at 700 to 1150 F by C. Mylonas and R. J. Beaulieu. April 1965.